

A combination of modeling and experimental approaches to investigate the novel nicotinothiazone Schiff base and its complexes with Zn(II) and ZrO(II) as inhibitors for mild-steel corrosion in molar HCl

Hany M. Abd El-Lateef^{a,b,*}, Kamal A. Soliman^c, Mohammed A. Al-Omair^a,
Mohamed Shaker S. Adam^{a,b}

^a Department of Chemistry, College of Science, King Faisal university, P.O. Box 400 Al-Ahsa 31982, Saudi Arabia

^b Chemistry Department, Faculty of Science, Sohag University, Sohag-82534, Egypt

^c Chemistry Department, Faculty of Science, Benha University, 13518 Benha, Egypt

ARTICLE INFO

Article History:

Received 31 December 2020

Revised 5 March 2021

Accepted 22 March 2021

Available online 29 March 2021

Keywords:

Nicotinothiazone Schiff base

Mild steel

Acid inhibition

Surface morphology

DFT

MC simulations

ABSTRACT

Two novel metal-complexes of 5-sodium sulfonate-2-hydroxybenzylidene)nicotinothiazone (H₂LCs) with Zn²⁺ and ZrO²⁺ ions were synthesized and characterized (ZnLCs and ZrOLCs), respectively. Condensation of nicotinothiazide with salicylaldehyde-5-sodium sulfonate salt afforded H₂LCs. Inhibition effectiveness of H₂LCs and its complexes with Zn(II) and Zr(II) for M-steel in a 1.0 M HCl solution was examined by electrochemical (E_{OCP} vs. time, impedance spectroscopy (EIS) and potentiodynamic polarization (PDP)) methods. In comparison with H₂LCs, ZnLCs and ZrOLCs display enhanced protection capacities. Particularly, the ZrOLCs compound displays higher protection power, and the efficacy is up to 97.4% at 5×10^{-4} mol L⁻¹ at 303 K. PDP studies exhibited that the as-prepared additives act as inhibitors of the mixed-kind, and adsorbed on M-steel surface via chemisorption following the Langmuir isotherm model. The surface morphology inspections (FE-SEM/EDX, and FT-IR) display that the M-steel interface was inhibited by titled compounds. To get a preferable comprehension of the adsorption of compound species on the steel interface, a detailed modeling investigation was accomplished using Monte Carlo (MC) simulation and DFT calculations. QSAR model also investigated via multiple linear regression method. The current report delivers very significant outcomes in designing and fabricating sustainable inhibitors with high protection capacity.

© 2021 Taiwan Institute of Chemical Engineers. Published by Elsevier B.V. All rights reserved.

1. Introduction

Mild steel (M-steel) has various applications in production and life due to its distinctive mechanical characteristics [1]. These comprise the manufacture of different containers, building components, furnaces, tanks, and agricultural equipment, as well as different heat transfer apparatus, heat exchange apparatus, and cooling equipment, etc. [2]. However, Corrosion of M-steel alloys causes enormous economic loss, particularly in oil-gas and petrochemical industries where acidic mediums are usually employed in several processes, e.g., cleaning, descaling, oil-well acidizing, and pickling implementations [3]. Hydrochloric acid is the most usually used pickling solution [4]. There is, however, the main hazard to use acidic mediums lacking further dealing with corrosion inhibitors because M-steel is roughly attacked by an acid corrosive medium. Consequently, the application of

inhibitors is a vital routine to safeguard the metals and alloys from corrosion in acid solutions [5,6].

The common of efficient inhibitors are usually carbon-based molecules that have single or more heteroatoms, sulfur, phosphorous, nitrogen, and oxygen, which performance as effective sites owing to their great electron density and high inclination to contribute electrons that ease the adsorption route on at steel/solution interface, thus shielding the metal from the corrosive attack and increasing the lifetime. The efficacy of organic compounds in the protection systems depends on how robust the additive is adsorbed on the steel interface and its adsorption is immediately connected to structural electronic properties, some physio-chemical advantages, the nature of the aggressive medium, and the metal surface charge [7,8]. It is well documented that nitrogen and sulfur-containing additives have exhibited superior protection than those containing individuals of these molecules. Newly, many reports on developing environmentally friendly, novel efficient, and harmless corrosion additives have become widespread. To the authors' preferable information,

* Corresponding author.

E-mail addresses: hmahmed@kfu.edu.sa, hany_shubra@science.sohag.edu.eg (H.M.A. El-Lateef).

RESEARCH ARTICLE

**A GEOMETRIC-MORPHOMETRIC ANALYSIS OF THE HETEROCHELY
IN THE RED SEA HERMIT CRAB “CLIBANARIUS SIGNATUS”, AND ITS
DEVELOPMENTAL STABILITY AND MODULARITY**

Tarek G. Ismail

Zoology Department, Faculty of Science, Sohag University, Sohag, Egypt

ABSTRACT

Article History:

Received: 25 May 2021

Accepted: 10 July 2021

Published Online:

11 July 2021

Keywords:

Developmental stability

Directional asymmetry

Fluctuating asymmetry

Geometrics morphometrics

Modularity

***Correspondence:**

Tarek G. Ismail

Zoology Department

Faculty of Science

Sohag University

Sohag, Egypt

E-mail:

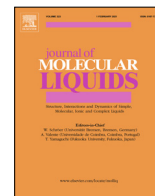
t_gad_2000@science.sohag.edu.eg

Geometric-morphometric analysis is growingly used to quantify/analyze biological forms and discriminate among subtle variation in shape. The hermit crab “*Clibanarius signatus*” showed subtle heterochely; therefore, geometric-morphometric analysis helps to determine visually these shape changes. Individuals of “*C. signatus*” were collected from a mangrove site on the Egyptian Red Sea coast. The present study aimed to: "1" detect the different types of asymmetries in *C. signatus* by geometrics morphometrics, "2" inspect the responsibility of occupied shell type on the chelae asymmetry, "3" investigate the asymmetry-types' differences between sexes, "4" use the fluctuating asymmetry as an indicator for developmental stability, "5" and to investigate morphological, developmental, and functional modularity in the chela compartments. Directional and fluctuating asymmetries were detected; both showed high size levels in the males than in the females. The males revealed a high-level of shape directional symmetry and low-level of shape fluctuating asymmetry compared with the females. All investigated individuals showed larger right chela. The fluctuating asymmetry may be attributed to developmental instability as a result of occupying dextral shells. The integration and modularity of the chela compartments revealed two developmental modules, which morphologically and functionally integrated as one module. The individual variation and the fluctuating asymmetry showed similar patterns indicating that the same developmental processes are contributed to the chela shape variation. The present results are indicative signs that environmental stress is present and sufficient to produce asymmetry in chelae size/shape. However, this asymmetry was subtle, suggesting that it does not produce notable variation in the chelae functions.

INTRODUCTION

Asymmetrical morphology in chelae (heterochely) of anomuran hermit crabs is well known with a larger right chela in Paguroidea and Parapaguridae or larger left

chela in the majority of Diogenidae, which also includes hermits with somewhat symmetrical chelae^[1]. The morphological features of chela parts in hermit crabs are related to prospective different functions



A novel approach to investigate the synergistic inhibition effect of nickel phosphate nanoparticles with quaternary ammonium surfactant on the Q235-mild steel corrosion: Surface morphology, electrochemical-computational modeling outlines

Ahmed O. Alnajjar^a, Hany M. Abd El-Lateef^{a,b,*}

^a Department of Chemistry, College of Science, King Faisal University, P.O. Box 380 Al Hofuf, 31982 Al-Ahsa, Saudi Arabia

^b Chemistry Department, Faculty of Science, Sohag University, Sohag 82534, Egypt

ARTICLE INFO

Article history:

Received 3 March 2021

Revised 1 April 2021

Accepted 8 April 2021

Available online 20 April 2021

Keywords:

Synergism
Nanoparticles
Corrosion protection
Theoretical modeling
Surface morphology
Electrochemical studies

ABSTRACT

Novel quaternary ammonium Surfactant, namely, *N,N*-dimethyl-*N*-(3-((2-nitrophenyl)sulfonamido)propyl)dodecan-1-aminium iodide (QAS-12) has been prepared and characterized. The inhibition performance of the individual QAS-12 surfactant and blended with nickel phosphate nanoparticles (NiPNPs) in 15% HCl on the Q235-mild steel was investigated by means of E_{OCP} - t profiles potentiodynamic, LPR corrosion rate and EIS measurements. The findings display that the corrosion rate of Q235-mild steel is considerably decreased with rise in the surfactant dose where the protection power of QAS-12 extends a maximum value of 93.1% at 0.5 mM. Synergistic protection effect was detected between the cationic QAS-12 and the NiPNPs additives, with the maximum protection capacity as high as ~98.6%. The adsorption behavior obeyed the Langmuir isotherm model with competitive of physical and chemical adsorption between the surfactant and metal. The individual surfactant and mixed with NiPNPs performed as mixed type inhibitors. Surface morphology analysis using XPS, SEM/EDX, and UV-vis absorption studies verified the high efficiency of the cationic surfactant on the inhibition of Q235-mild steel in 15% HCl solution, and the synergistic effect on corrosion protection among the QAS-12 and the NiPNPs was confirmed. Correlation of Computational Modeling with empirical findings of the current work is discussed based on the DFT calculations and MC simulation. The proposed mechanism for the synergism resulting from both addition of the cationic surfactant and NiPNPs was also discussed according to the obtained outcomes.

© 2021 Elsevier B.V. All rights reserved.

1. Introduction

Steel alloys are a significant class of materials, which have been extensively applied in multiple critical industries, including petroleum, machinery, construction, transportation and storage. Acidic mediums are widely used in various fields processes for example pickling, cleaning, descaling and acidizing to eliminate rust and scales on steel alloy surfaces [1,2]. Acid solutions such as HCl or H₂SO₄ are generally employed as pickling agents, which, nevertheless, as well cause intensive corrosion to steel alloys, and lead to not only remarkable financial loss but also critical integrity matters [3]. Accordingly, the solutions of pickling processes are regularly encouraged with appropriate corrosion inhibitors with the inten-



tion of protect the steel alloys from corrosion during pickling procedures [4,5]. Previously, substantial consideration has been paid for protection of steel alloys corrosion in different corrosive solutions [6–8].

Corrosion inhibitors could be separated into 3-kinds based on their chemical structures: organic, inorganic and mixed-type inhibitors [9,10]. Inorganic material inhibitors like nitrite, phosphate, borate, and chromate, could produce an impermeable film on the steel surface to restrain the corrosive medium; however, they are generally extremely toxic and cause abundant damage to the environment [11]. Instead, organic inhibitors which comprise heteroatoms (nitrogen, oxygen, sulphur or phosphorus), aromatic rings, or electron lone pairs are frequently fewer toxic and have been the most extensively utilized corrosion inhibitors [12–14]. Organic inhibitors could adsorb onto metal interfaces via chemisorption and/or physisorption. The physisorption frequently depend on the electrostatic attraction among the charged electrode surface and the charged inhibitors, while the chemisorption depend on

* Corresponding author at: Department of Chemistry, College of Science, King Faisal University, P.O. Box 380 Al Hofuf, 31982 Al-Ahsa, Saudi Arabia.

E-mail addresses: hmahmed@kfu.edu.sa (A.O. Alnajjar), hany_shubra@science.sohag.edu.eg (H.M. Abd El-Lateef).

A Pilot Study of Smart Agricultural Irrigation using Unmanned Aerial Vehicles and IoT-Based Cloud System

Mohamed Esmail Karar ^{1,2} , Faris Alotaibi ¹, Abdullah AL Rasheed ¹, Omar Reyad ^{1,3} 

¹ College of Computing and Information Technology, Shaqra University, Saudi Arabia

² Faculty of Electronic Engineering, Menoufia University, Egypt

³ Faculty of Science, Sohag University, Egypt

mkarar@su.edu.sa; S437460268@su.edu.sa; S437460255@su.edu.sa; oreyad@su.edu.sa

Abstract—This article introduces a new mobile-based application of modern information and communication technology in agriculture based on Internet of Things (IoT), embedded systems and an unmanned aerial vehicle (UAV). The proposed agricultural monitoring system was designed and implemented using Arduino microcontroller boards, Wi-Fi modules, water pumps and electronic environmental sensors, namely temperature, humidity and soil moisture. The role of UAV in this study is to collect these environmental data from different regions of the farm. Then, the quantity of water irrigation is automatically computed for each region in the cloud. Moreover, the developed system can monitor the farm conditions including the water requirements remotely on Android mobile application to guide the farmers. The results of this study demonstrated that our proposed IoT-based embedded system can be effective to avoid unnecessary and wasted water irrigation within the framework of smart agriculture.

Keywords—Internet of things, precision agriculture, embedded systems, cloud computing, smart irrigation, Agricultural drone

1. Introduction

Water is one of essential natural resources for agriculture. Most growing population in the world is relying on agriculture and consumes about 56.0 % of the fresh water globally [1]. However, water availability for irrigation is currently limited because of climate change and other environmental factors such as decreasing groundwater resources, while increasing industrial and domestic demands [2]. Additionally, a large amount of irrigation water is always wasted and cannot be managed efficiently because of traditional irrigation methods to achieve expected crop productivity. Therefore, design and development of smart water irrigation systems become an attractive topic for many researchers because of its potential outcome to achieve sustainable agriculture [3, 4].

Smart agriculture or precision agriculture provides an application of modern and accurate information and communications technology to automate and optimize difficult agricultural tasks and/or processes [5, 6]. Internet of Things (IoT) presents the core networking technology of smart agriculture and many recent wireless applications ranging from environment monitoring to healthcare and medical applications [7-11]. In smart agriculture, IoT is used to collect data from sensors which measure different parameters such as soil moisture and humidity and monitor them remotely via developed mobile applications to take decisions or to actuate devices, e.g., water pumps [6]. Consequently, the workload of the farmers will be reduced with efficient use of available resources and low-cost appliances. Artificial intelligence (AI) techniques can be also applied to analyze agricultural and environmental data to support the specialists and farmers; for example, machine learning including neural networks [12], fuzzy logic controllers [13], and recently deep learning models [14]. However, continuous screening and monitoring of the crops, automated water irrigation, and plant disease detection are still main challenges of smart agriculture, as depicted in Fig. 1 [6, 15]. In this study, we will focus only on proposing two solutions for the challenges of continuous monitoring of the field and automatic irrigation using IoT and unmanned aerial vehicles (UAVs).



A promising star-like PtNi and coral reefs-like PtCo nano-structured materials for direct methanol fuel cell application

Mansour Sadek^a, Hany M. Abd El-Lateef^{a,b,*}, Hossnia S. Mohran^a, Mahmoud Elrouby^{a,*}

^a Chemistry Department, Faculty of Science, Sohag University, Sohag 82524 Egypt

^b Department of Chemistry, College of Science, King Faisal University, P.O. Box 400 Al-Ahsa 31982, Saudi Arabia

ARTICLE INFO

Article history:

Received 20 March 2021

Revised 3 September 2021

Accepted 30 September 2021

Available online 5 October 2021

Keywords:

Electrochemical synthesis
PtNi and PtCo nanostructured
Electrocatalytic oxidation
DMFC

ABSTRACT

Novel composite catalysts of nanostructured PtCo and PtNi alloys onto a coated glassy carbon electrode (GCE) with a nanostructured alloy of NiCo as a substrate material were fabricated by an electrodeposition method from their salt solutions at ambient temperature. The PtCo/NiCo/GCE and the PtNi/NiCo/GCE catalysts display an improved electrocatalytic behavior for the electrochemical oxidation reaction of methanol (MOR). The morphology, chemical composition, and phase structure for the electrodeposited catalysts were checked utilizing a scanning electron microscope (SEM), energy-dispersive X-ray spectroscopy (EDAX), and X-ray diffraction (XRD) technique, respectively. PtCo/NiCo/GCE catalyst shows coral particles of reef-shaped morphology, whilst the PtNi/NiCo/GCE catalyst star-shaped particles. The electrocatalytic performance of the electrodeposited catalysts was verified using chronoamperometry and cyclic voltammetry (CV). The effects of the type of electrodeposition method, pH of the solution, temperature, and precursors concentration on the characteristics of the PtCo and PtNi alloys electrodeposits and accordingly on the electrocatalytic peculiarities of the catalysts were well assessed. Furthermore, the impact of methanol concentration and temperature on MOR was discussed. The stability and the corrosion resistance tests of the PtNi/Ni-Co/GCE and PtCo/Ni-Co/GCE systems were evaluated via the electrochemical impedance spectroscopy (EIS), Tafel polarization, and potentiostatic methods.

© 2021 Elsevier Ltd. All rights reserved.

1. Introduction

Energy has become a basic need of modern society in all-imaginable dimensions. Carbon, natural gas, and petroleum are the master sources of energy. The combustion of fossil fuels releases harmful emissions like NO_x, SO_x, CO₂, and particulate matter, which is a major concern for environmental pollution. Over and above that these fossil fuels being non-renewable, their possible extinction causes a major threat to the standard of living. Renewable energy sources like solar, wind, etc., may be a possible solution, but these sources might not be suited to cover the current energy demand. Fuel cells are now appreciated as a favorable solution to future energy dilemmas. This is because they are smart devices that transform the chemical energy of a fuel into electrical energy via an electrochemical oxidation reaction without combustion [1–3].

Fuel cells can be classified into many types according to the used fuel and membrane, such as the solid oxide (SOFC), phosphoric acid (PAFC), polymer electrolyte membrane (PEMFC), molten carbonate (MCFC), alkaline (AFC), and direct methanol (DMFC). The DMFC is a suitable power source for portable mobile electronic devices and electric vehicles [4]. The vital merit of this sort of cell is the liquid methanol utilized as a fuel has been easy storage and transportation than hydrogen gas fuel, which faces a flammability and storage problem [5]. Furthermore, the methanol fuel doesn't need prior reforming process requirements, compared to the hydrogen gas fuel [6]. Moreover, methanol fuel has a higher energy density (4820 Wh L⁻¹) than the fuel of hydrogen gas (180 Wh L⁻¹) [7]. The utilized material as electrocatalyst for the DMFC should comprise of two basic portions; a) the alloys or metal which activates the main reaction and b) the supportive material, which facilitates the metal particles distribution on its surface providing a high surface area for accomplishment the reaction. Although, a few difficulties still frustrate its trading in markets. One of the significant difficulties is that the utilized Pt as catalyst exhibits some electron transfer relaxation towards the electro-oxidation reaction of methanol, which is due to the self-poisoning for the surface of Pt catalyst. This poisoning is attributed to the strong adsorption of

* Corresponding author at: Chemistry Department, Faculty of Science, Sohag University, Sohag 82524 Egypt.

E-mail addresses: hany_shubra@science.sohag.edu.sa (H.M. Abd El-Lateef), dr_mahmoudelerouby@science.sohag.edu.eg (M. Elrouby).



A Study of Photo-Thermoelastic Wave in Semiconductor Materials with Spherical Holes Using Analytical-Numerical Methods

Faris S. Alzahrani¹ · Ibrahim A. Abbas^{1,2}

Received: 12 March 2021 / Accepted: 25 May 2021
© Springer Nature B.V. 2021

Abstract

Analytical and numerical solutions are two basic tools in the study of photothermal interaction problems in semiconductor medium. In this paper, we compare the analytical solutions with the numerical solutions for thermal interaction in semiconductor mediums containing spherical cavities. The governing equations are given in the domain of Laplace transforms and the eigenvalues approaches are used to obtain the analytical solution. The numerical solutions are obtained by applying the implicit finite difference method (IFDM). A comparison between the numerical solutions and analytical solution are presented. It is found that the implicit finite difference method (IFDM) is applicable, simple and efficient for such problems.

Keywords Finite difference method · Semiconductor material · Laplace transforms · Spherical cavity · Eigenvalues scheme

Nomenclature

$N = n - n_o, n_o$	the carrier concentration at equilibrium,
$\gamma_n = (3\lambda + 2\mu)d_n$	the electronic deformation coefficient,
d_n	
$\delta = \frac{\partial n_o}{\partial T}$	the coupling parameter of thermal activation
K	the thermal conductivity
$\gamma_t = (3\lambda + 2\mu)\alpha_t$	the linear thermal expansion coefficients
α_t	
c_e	the specific heat at constant strain,
τ	the lifetime of photo-generated carrier,
σ_{ij}	the components of stresses,
D_e	the carrier diffusion coefficient,
λ, μ	the Lamé's constants,
$T = T^* - T_o, T^*$	the variations of temperature
T_o	the reference temperature
t	the time
t_f	the final value of time

x_f	the final value of length
s_b	the speed of recombination on the surface
u_i	the displacement components
ρ	the density of material
T_1	the constant temperature
Ω	the exponent of the decayed heat flux

1 Introduction

In the surrounding nature, many materials are very important in industry especially, these materials have many applications in renewable energy. The semiconductor materials exist in abundance in the surrounding nature which have great economic importance in solar cells industry. When the semiconductor media are exposed to a focus of laser beams or a beam of sunlight, the surface electrons at free surface are thermally excited and they will be vibrated due to the thermal effect of laser beams. In this case, the electrons and holes will transport from one position to another and the free carriers photo-excited appearing with a weak electrical current.

On the other hand, the recombination processes during the photo-excited processes will be taken into account between the electrons (carrier density (plasma)) and holes. Much effort has been made for generalized theories of thermoelasticity in solving thermoelastic models instead of the classical

✉ Ibrahim A. Abbas
ibrabbas7@yahoo.com; ibrabbas7@science.sohag.edu.eg

Faris S. Alzahrani
falzahrani1@kau.edu.sa

¹ Department of Mathematics, Faculty of Science, King Abdulaziz University, Jeddah, Saudi Arabia

² Department of mathematics, Faculty of Science, Sohag University, Sohag, Egypt

A study on thermo-elastic interactions in 2D porous media with-without energy dissipation

Faris Alzahrani¹ and Ibrahim A. Abbas^{*1,2}

¹Nonlinear Analysis and Applied Mathematics Research Group (NAAM), Mathematics Department,
King Abdulaziz University, Jeddah, Saudi Arabia

²Department of Mathematics, Faculty of Science, Sohag University, Sohag, Egypt

(Received September 25, 2020, Revised January 29, 2021, Accepted February 14, 2021)

Abstract. The generalized thermoelastic analysis problem of a two-dimension porous medium with and without energy dissipation are obtained in the context of Green–Naghdi's (GNIII) model. The exact solutions are presented to obtain the studying fields due to the pulse heat flux that decay exponentially in the surface of porous media. By using Laplace and Fourier transform with the eigenvalues scheme, the physical quantities are analytically presented. The surface is shocked by thermal (pulse heat flux problems) and applying the traction free on its outer surfaces (mechanical boundary) through transport (diffusion) process of temperature to observe the analytical complete expression of the main physical fields. The change in volume fraction field, the variations of the displacement components, temperature and the components of stress are graphically presented. Suitable discussion and conclusions are presented.

Keywords: Porous medium; fourier and laplace transform; eigenvalue approach; Green–Naghdi (GNIII) theory

1. Introduction

The models of linear elastic materials with voids are a significant generalization of the classical models of elastic materials. These models are used to study various types of geological and biological materials for which the classical models are not sufficient. Porous mediums make their apparition in wided forms of environment, natural and synthetic and in several implementations of technology. An elastic medium with voids is basically porous media whose skeletons (matrices) are an elastic solid and the interstices is void (small pore) containing nothing of energetic and physical significances. The models of linear elastic mediums with voids treat materials with a small or empty pore distribution, where the void volume is included among the kinematic variables. These theories are reduced to the classical theories in the limit cases of the voids volume tending to zeros. The field of thermoelasticity was first stimulated by the work of Biot (1941, 1956). Green and Naghdi (1991), Green and Naghdi (1993) established new generalized thermo-elastic theory by including the thermal displacement gradient between the independent constitutive variable. (Othman and Abbas 2012) have discussed the generalized thermoelastic problem with energy dissipation in a non-homogeneous isotropic hollow cylinder. Kumar *et al.* (2016) investigated the thermomechanical interactions subjected to hall current under GNIII model with two-

temperatures and rotations in thermoelastic transversely isotropic medium. Othman and Marin (2017) applied normal modes approach to investigate the effect of GN model in thermoelastic porous media due to laser pulse. Abbas (2006) discussed the natural frequency of a poro-elastic cylinder. Marin and Öchsner (2017) investigated the effects of a dipolar structures with Green and Naghdi thermoelasticity theory. Karageorghis *et al.* (2014) discussed the movable pseudo-boundaries MFS for voids detection in two-dimension thermoelastic material. Sur and Kanoria (2019) studied the effect of memory on thermoelastic waves propagation in solid with voids. Many researchers (Milani Shirvan *et al.* 2017, Milani Shirvan *et al.* 2017; Ellahi *et al.* 2019; Marin *et al.* 2019, Sheikholeslami *et al.* 2019, Zeeshan *et al.* 2019) have presented the solutions of many problems for porous mediums with several boundary conditions. The authors (Abbas and Youssef 2009, Mohamed *et al.* 2009, Othman and Abbas 2011, Abbas and Youssef 2013, Abbas 2014, Sur and Kanoria 2014, Zenkour and Abbas 2014, Sharma *et al.* 2015, Abbas and Alzahrani 2016, Abbas and Kumar 2016, Lata *et al.* 2016, Ezzat and El-Bary 2017, Ezzat and El-Bary 2017, Eftekhari 2018, Kahya and Turan 2018, Lata 2018, Itu *et al.* 2019; Lata and Kaur 2019, Mondal *et al.* 2019, Othman and Mondal 2019, Sarkar and Mondal 2019, Vlase *et al.* 2019, Kaur and Lata 2020, Mondal and Othman 2020, Sur, Mondal *et al.* 2020) studied the solutions of many problems under generalized thermo-elastic theories. In the domains of Laplace, the eigenvalue method gave the analytical solutions without any supposed restriction on the factual physical quantities as in (Alzahrani and Abbas 2016, Alzahrani and Abbas 2018). Abbas (2014) presented the solution of nonlinear transient thermal stresses in a thick-walled FGM cylinder under temperature-dependent

*Corresponding author, Professor

E-mail: ibrabbas7@gmail.com

^aProfessor

E-mail: falzahrani1@kau.edu.sa



A synergetic effect of cerium oxide nanocubes and gold nanoparticles for developing a new photoelectrochemical sensor of codeine drug



Mohamed Khairy

Chemistry Department, Faculty of Science, Sohag University, Sohag, 82524, Egypt

ARTICLE INFO

Keywords:

Photoelectrochemical sensor
Codeine
Screen-printed electrode
Cerium oxide nanocubes
Gold nanoparticles
Legal-high drugs

ABSTRACT

A new photoelectrochemical sensor for codeine (COD) drug based on cerium oxide nanocubes (NCs) and gold nanoparticles (NPs) composite modified screen-printed electrode (SPE) is developed for the first time. Codeine belongs to the opiates drug family naturally found in the poppy plant, has intensive effects on the central nervous system. Although CeO₂ NCs showed a photoelectrochemical signal, the combination with Au NPs significantly improves the sensitivity four times and selectivity toward COD. Further, the synergetic combination of CeO₂ NCs/Au NPs allows the generation of photocurrent extended to the visible light region because it sensitizes charge carrier generation. The CeO₂ NCs/Au NPs -SPE offers a promising, robust, and chemically stable non-enzymatic photoelectrochemical sensor for COD determination within a linear detection range up to 200 μM and a lower detection limit (LOD) (3S/N) of 0.02 μM. The proposed PECS showed high stability and good reproducibility which extend the applicability to generate a new monitoring system for in-set drug analysis.

1. Introduction

Codeine (COD) is chemically known as 3-methyl morphine or 7,8-dihydro-4,5-epoxy-3-methoxy-17-methylmorphinan-6-ol monohydrate. It is an alkaloid opiate naturally found in the poppy plant [1]. It is a narcotic prodrug metabolized by the liver enzyme CYP2D6 to active morphine via *o*-demethylation. It is often used for the treatment of mild and moderate pain in adults and children [2]. COD is one of the most opiate drugs used in the world and listed by the World Health Organization (WHO) in 2017 as an essential medicine needed for the basic health system although it potentially affects the central nervous system [3]. It might cause drug addiction and mental damage if abused. The intensive medication of COD leading to depression, sedation, and miosis, nausea, vomiting, skeletal muscle flaccidity, bradycardia, hypotension in addition to apnea, or even death [4]. As a result, the development of a low-cost, sensitive, and selective analytical tool for COD monitoring is urgently needed to consider the growing health and public security. High-performance liquid chromatography (HPLC) [5], gas chromatography (GC) [6], capillary electrophoresis (CE) [7], spectrofluorimetry [8], and electrochemistry [9,10] were explored for COD determination. Among these methods, electrochemistry offers an easy-to-use strategy with high accuracy and selectivity in complex samples without the time-consuming or necessity of skilled personnel [11]. Recently, the integration of

electrochemistry and light illumination is a promising concept to enhance the analytical features of biosensors [12].

Photoelectrochemical sensing is an attractive tool used recently for rapid and accurate monitoring of chemical and biochemical molecules [13,14]. The construction of photoelectrochemical platforms is based on a fruitful integration of traditional electroanalytical techniques with photo-excited semiconductor materials followed by measurement of the electron transfer reactions at the electrode/electrolyte interface. Under light illumination, the photoactive semiconductor materials generate charge carriers (holes/electrons pairs) which subsequently migrate to valance and conduction band edges under the influence of the electric field, respectively. Otherwise, the photo-generated charge carriers recombine again immediately in the bulk. The photo-generated charge carrier holes/electrons could be utilized for the oxidation/reduction reactions of the analyte. While the remaining opposite photo-generated charge transfer to back contact and triggers photocurrent [12]. Thus, photoelectrochemical sensing is a unique technique widely used in the last decade for biology, medicine, and environmental fields due to potentially higher sensitivity and selectivity compared to conventional electrochemical and chemiluminescent methods. Additionally, it also offers simple instrumentation, low cost, and easy to miniaturize compared to spectroscopy techniques. However, the engineering of photoactive materials to meet the growing sensing demand is still the most crucial step for the development of photoelectrochemical platforms.

E-mail address: mohamed.khairy@science.sohag.edu.eg

<https://doi.org/10.1016/j.jelechem.2021.115517>

Received 8 March 2021; Received in revised form 20 June 2021; Accepted 6 July 2021

Available online 9 July 2021

1572-6657/© 2021 Elsevier B.V. All rights reserved.



Acid rain induced leakage of Ca, Mg, Zn, Fe from plant photosynthetic organs – Testing for deciduous and dicotyledons

Jean Diatta^{a,*}, Naglaa Youssef^b, Oskar Tylman^c, Witold Grzebisz^a, Bernd Markert^d, Leszek Drobek^e, Simone Wüenschmann^d, Małgorzata Bebek^e, Krzysztof Mitko^e, Paweł Lejwoda^e

^a Poznan University of Life Sciences, Department of Agricultural Chemistry and Environmental Biogeochemistry, ul. Wojska Polskiego 71F, 60-625, Poland

^b Department of Botany and Microbiology, Faculty of Science, Sohag University, Sohag 82524, Egypt

^c Poznan University of Life Sciences, Department of Soil Science and Land Protection, 60-656 Poznań, ul. Szydlowska 50, Poland

^d Environmental Institute of Scientific Networks, Fliederweg 17, 49733 Haren/Erika, Germany

^e Central Mining Institute, Department of Environment Monitoring, Plac Gwarkow 1, 40-166 Katowice, Poland

ARTICLE INFO

Keywords:

Acid rain
Mineral leakage
Deciduous trees
Dicotyledonous plants
Mineral photosynthetic index
Vulnerability
Resistance

ABSTRACT

Simulated acid rains (AR), (pH 3.0, 3.5, 4.0, 4.5, 5.0, 5.5) were applied to green leaves of 13 deciduous trees (DT) and 10 species of dicotyledonous plants (DP). All were incubated at 23 °C within a growth chamber for 72 h. After the contact time, the leachates were analyzed for pH and next mineral elements: Ca, Mg, Fe, Zn. Total leaf concentrations of Ca and Mg have exhibited different relationships with $Mg_{(DT)} = 6.85Ca_{(DT)}^{0.566}$, $R^2 = 0.64$ and $Mg_{(DP)} = 0.079Ca_{(DP)} + 318.8$, $R^2 = 0.41$. Leakage process revealed that intra-species variation for DT follows: Mg (107.3%) > Ca (106.0%) > Zn (90.3%) > Fe (59.8%), implying that the leaking effect was much more pronounced for alkaline elements (Ca, Mg). Dicotyledonous plants (DP), displayed a similar pattern but less varied: Mg (78.7%) > Ca (75.6%) > Zn (66.5%) > Fe (55.8%). The elaborated mineral photosynthetic index (MPI), $[Mg/(Zn + Fe)]$ revealed that 77% of deciduous species represented very low to intermediate photosynthetic recovery, meaning that highly acid rain impacted trees will be surviving less or none. High DT survivors should be maple, linden and hornbeam. Dicotyledonous plants (DP) covered 70% of high to very high survival feature, where cucumber, cabbage and daisy prevailed.

We stipulate that regreening of zones endangered by acid rains or planning green urban spaces should consider tree species with much more higher Ca concentrations in leaves. Both Ca^{2+} and Mg^{2+} intracellular hydrolysis appears as an efficient buffer inactivating acidity.

1. Introduction

Acid rain (AR) has been regarded as one of the three severest environment disasters facing mankind today around the world (Larssen et al., 2006; Xu et al., 2015). The major sources of AR are sulfur dioxide (SO₂) and nitrogen oxides (NO_x) emitted into the atmosphere. When these oxides react with water in the atmosphere, sulfuric and nitric acids can form and fall as rains (Jalali and Naderi, 2012). These oxides mainly come from anthropogenic activities, such as coal combustion, power plants, and car traffic (Liu et al., 2016). The precipitations with pH values lower than 5.6 have been defined as AR, which has contributed to several key environmental issues, including acidification of soils and waters, leaf injury and forest decline, loss of biodiversity, and damage of buildings and metal materials (Ramlall et al., 2015; Ju et al., 2017).

As the main part of the terrestrial ecosystems, plants can be considered as the biggest victim of AR pollution (Ramlall et al., 2015). AR directly suppresses leaf function by eroding surface waxes and cuticle and leaching base cations from mesophyll cells (Dong et al., 2017; Du et al., 2017; Wu and Liang, 2017). The more acute injury of AR to plant foliage includes reduction in photosynthetic rate, variation in stomatal conductance, and decrease in chlorophyll content (Dong et al., 2017; Du et al., 2017). In addition, AR accelerates the leaching of nutrients (Ca, Mg, K, and Na) from leaves which leads to the abnormal or restricted growth (Ju et al., 2017; Wu and Liang, 2017). It leads to further decreases in vertical growth, stem incremental growth, and in total plant biomass (Zhang et al., 2016; Wu and Liang, 2017; Liu et al., 2018).

Reports of Dai et al. (2013); Qiu et al. (2015) showed that AR is able

* Corresponding author.

E-mail address: jean.diatta@up.poznan.pl (J. Diatta).

<https://doi.org/10.1016/j.ecolind.2020.107210>

Received 22 May 2020; Received in revised form 12 October 2020; Accepted 22 November 2020

Available online 8 December 2020

1470-160X/© 2020 Published by Elsevier Ltd. This is an open access article under the CC BY-NC-ND license (<http://creativecommons.org/licenses/by-nc-nd/4.0/>).

Article

An Intelligent Metaheuristic Binary Pigeon Optimization-Based Feature Selection and Big Data Classification in a MapReduce Environment

Felwa Abukhodair ¹, Wafaa Alsaggaf ¹, Amani Tariq Jamal ², Sayed Abdel-Khalek ^{3,4}
and Romany F. Mansour ^{5,*}

¹ Department of Information Technology, Faculty of Computing and Information Technology, King Abdulaziz University, Jeddah 21589, Saudi Arabia; felwaabukhodair@gmail.com (F.A.); waalsaggaf@kau.edu.sa (W.A.)

² Department of Computer Science, Faculty of Computing and Information Technology, King Abdulaziz University, Jeddah 21589, Saudi Arabia; Atjamal@kau.edu.sa

³ Department of Mathematics and Statistics, College of Science, Taif University, P.O. Box 11099, Taif 21944, Saudi Arabia; sayedquantum@yahoo.co.uk

⁴ Department of Mathematics, Faculty of Science, Sohag University, Sohag 82524, Egypt

⁵ Department of Mathematics, Faculty of Science, New Valley University, El-Kharga 72511, Egypt

* Correspondence: romanyf@sci.nvu.edu.eg

Abstract: Big Data are highly effective for systematically extracting and analyzing massive data. It can be useful to manage data proficiently over the conventional data handling approaches. Recently, several schemes have been developed for handling big datasets with several features. At the same time, feature selection (FS) methodologies intend to eliminate repetitive, noisy, and unwanted features that degrade the classifier results. Since conventional methods have failed to attain scalability under massive data, the design of new Big Data classification models is essential. In this aspect, this study focuses on the design of metaheuristic optimization based on big data classification in a MapReduce (MOBDC-MR) environment. The MOBDC-MR technique aims to choose optimal features and effectively classify big data. In addition, the MOBDC-MR technique involves the design of a binary pigeon optimization algorithm (BPOA)-based FS technique to reduce the complexity and increase the accuracy. Beetle antenna search (BAS) with long short-term memory (LSTM) model is employed for big data classification. The presented MOBDC-MR technique has been realized on Hadoop with the MapReduce programming model. The effective performance of the MOBDC-MR technique was validated using a benchmark dataset and the results were investigated under several measures. The MOBDC-MR technique demonstrated promising performance over the other existing techniques under different dimensions.

Keywords: big data; metaheuristics; feature selection; Hadoop; MapReduce; data classification



Citation: Abukhodair, F.; Alsaggaf, W.; Jamal, A.T.; Abdel-Khalek, S.; Mansour, R.F. An Intelligent Metaheuristic Binary Pigeon Optimization-Based Feature Selection and Big Data Classification in a MapReduce Environment. *Mathematics* **2021**, *9*, 2627. <https://doi.org/10.3390/math9202627>

Academic Editor: Bogdan Oancea

Received: 23 September 2021

Accepted: 15 October 2021

Published: 18 October 2021

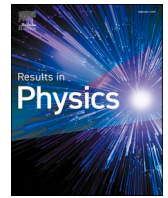
Publisher's Note: MDPI stays neutral with regard to jurisdictional claims in published maps and institutional affiliations.



Copyright: © 2021 by the authors. Licensee MDPI, Basel, Switzerland. This article is an open access article distributed under the terms and conditions of the Creative Commons Attribution (CC BY) license (<https://creativecommons.org/licenses/by/4.0/>).

1. Introduction

The term Big Data (BD) represents a huge amount of information [1], which can be unstructured and structured. With regards to data processing, the great significance is the organization that employs this information [2]. Nowadays, it can be extensively employed for outperforming peers and can be determined as variety, volume, and velocity. Variety refers to the data being structured or unstructured, volume refers to the amount of data produced, and velocity refers to the speed at which the data are being generated at. The significant advantages of BD are cost and time savings, large data processing, forecasting and analysis, and efficacy because of an innovative tool support [3]. The adoption of data mining (DM) tools to solve BD problems might require the remodeling of the algorithm and its inclusion in parallel environments. Amongst the distinct alternatives is the MapReduce (MR) model [4] and its distributed file systems, first presented by Google, which provides



Analysis and control of a fractional chaotic tumour growth and decay model

Emad E. Mahmoud^{a,b,*}, Lone Seth Jahanzaib^c, Pushali Trikha^c, Kholod M. Abualnaja^d

^a Department of Mathematics and Statistics, College of Science, Taif University, P.O. Box 11099, Taif 21944, Saudi Arabia

^b Department of Mathematics, Faculty of Science, Sohag University, Sohag 82524, Egypt

^c Department of Mathematics, Jamia Millia Islamia, New Delhi 110025, India

^d Department of Mathematics, Umm Al-Qura University, P.O. Box 14949, Makkah, Saudi Arabia

ARTICLE INFO

Keywords:

Tumour model
Fractional chaotic system
Adaptive sliding mode control
Chaos control
Dynamical analysis

ABSTRACT

In the manuscript fractional tumour growth and decay model is studied extensively using various dynamic analysis methods such as Lyapunov exponents, bifurcation and fixed point analysis, solution and so on. The model dynamics is observed by changing order between 0.8 and 1. Chaos has been observed in this fractional tumour growth and decay model. The model is also stabilized about its equilibrium points by chaos control technique using adaptive sliding mode control scheme. Numerical simulations are carried out to validate the theoretical results. These observations may prove fruitful and provide insight to deal with the disease.

Introduction

When we study the tumour system, a lot of complexities are found which are because of the diversity of the stages of tumour system, various time scales of each stage, tumour environment and tumour immune interactions [14] [15] [16]. Because of this complexity various types of attractors such as double wing, multi wing, limit cycle and strange attractor emerges [19]. These types of behavior lead to the complex dynamics of the tumour systems [17] [18] and can be addressed using the properties of chaos, like high dependence on initial conditions is the reason for different patterns of tumour growth found among various individuals. This is a very big challenge for the oncologist to deal with. In this scenario chaos theory could prove to be a very powerful tool to deal with this challenge. Treatment may include some techniques of chaos control, chaos synchronization [21,10–13] and anti-control of chaos.

In the study of understanding and analyzing chaos, focus has been shifted to control chaos and utilize it for various purposes. Chaos control involves stabilizing the chaotic system about some equilibrium points. Various chaos controlling technique have been developed such as optimal control technique [26], passive control [24] [25], impulsive control [27] etc. These control techniques have been used in various variety of application like medicine, biology [34] [37], physics [36],

engineering [28] [29] [35]. With emerging of fractional calculus in the area of research in recent years, it has opened new fields in both theories and applications. These days modeling of fractional differential equations have attained a great significance in the numerous real world problems of many fields such as biology, physics, engineering and many others [30] [31]. As the fractional order chaotic systems have the advantage of having an extra parameter, this gives an additional dimension in study of various chaotic models [32] [33] making it applicable across various disciplines. Nowadays many diseases are rapidly growing across the world and heavily affecting our health care system. Cancer is one among them which is taking a toll on the masses all over the world. But the general understanding of the prevention methods, causes and cure are still in its nascent stage. Mathematical modelling has shown the potential to provide better understanding for such complex biological systems [4] [5] [6] [7]. These mathematical models provide us the explanation of many phenomena observed and also provide insight into many unobservable phenomena [8] [9]. Various modeling methods to describe the dynamics of tumour growth have been studied and proposed. One of the commonly used and popular model is the exponential growth model, which takes into account that condition that the growth of tumour increases exponentially without any capacity constraints until the death of the patient. But it does not work for the large tumours considering the vascularity and the

* Corresponding author at: Department of Mathematics and Statistics, College of Science, Taif University, P.O. Box 11099, Taif 21944, Saudi Arabia.
E-mail addresses: e.mahmoud@tu.edu.sa (E.E. Mahmoud), lone179708@st.jmi.ac.in (L.S. Jahanzaib), pushali179707@st.jmi.ac.in (P. Trikha), kmaboualnaja@uqu.edu.sa (K.M. Abualnaja).

<https://doi.org/10.1016/j.rinp.2020.103677>


Received 30 October 2020; Received in revised form 25 November 2020; Accepted 27 November 2020

Available online 10 December 2020

2211-3797/© 2020 The Author(s). Published by Elsevier B.V. This is an open access article under the CC BY license (<http://creativecommons.org/licenses/by/4.0/>).

Article

Analysis of Genetic Diversity and Population Structure in Bitter Gourd (*Momordica charantia* L.) Using Morphological and SSR Markers

Ahmad Alhariri ^{1,2,*} , Tusar Kanti Behera ^{1,*}, Gograj Singh Jat ^{1,*}, Mayanglambam Bilashini Devi ³, G. Boopalakrishnan ¹, Nada F. Hemeda ⁴ , Ayaat A. Teleb ⁴, E. Ismail ⁵ and Ahmed Elkordy ^{6,7} 

- ¹ Division of Vegetable Science, ICAR-Indian Agricultural Research Institute, Pusa Campus, New Delhi 110012, India; gbkishnan85@gmail.com
- ² Faculty of Agriculture, Damascus University, Damascus 30621, Syria
- ³ ICAR-Research Complex for North Eastern Hilly Region, Umiam 793103, India; bilashini1712@gmail.com
- ⁴ Department of Genetics, Faculty of Agriculture, Fayoum University, Fayoum 63511, Egypt; nfh00@fayoum.edu.eg (N.F.H.); aat01@fayoum.edu.eg (A.A.T.)
- ⁵ Genetics Department, Agriculture Faculty, University of Sohag, Sohag 82524, Egypt; emad.eldeen.ismail1976@gmail.com
- ⁶ Biodiversity and Environment Management Department, Faculty of Biological and Environmental Sciences, University of Leon, 24071 Leon, Spain; aelkordy@science.sohag.edu.eg
- ⁷ Botany and Microbiology Department, Faculty of Science, University of Sohag, Sohag 82524, Egypt
- * Correspondence: ahmadharere@yahoo.com (A.A.); tusar@rediffmail.com (T.K.B.); singhgograj@gmail.com (G.S.J.)



Citation: Alhariri, A.; Behera, T.K.; Jat, G.S.; Devi, M.B.; Boopalakrishnan, G.; Hemeda, N.F.; Teleb, A.A.; Ismail, E.; Elkordy, A. Analysis of Genetic Diversity and Population Structure in Bitter Gourd (*Momordica charantia* L.) Using Morphological and SSR Markers. *Plants* **2021**, *10*, 1860. <https://doi.org/10.3390/plants10091860>

Academic Editor: Calvin O. Qualset

Received: 18 August 2021

Accepted: 4 September 2021

Published: 8 September 2021

Publisher's Note: MDPI stays neutral with regard to jurisdictional claims in published maps and institutional affiliations.

Abstract: The present investigation was carried out using 51 diverse bitter gourd accessions as material for studying genetic diversity and relatedness using morphological and SSR markers. A wide variation was observed for morphological traits like the number of days to the first female flower anthesis (37.33–60.67), the number of days to the first fruit harvest (47.67–72.00), the number of fruits/plant (12.00–46.67), fruit length (5.00–22.23 cm), fruit diameter (1.05–6.38 cm), average fruit weight (20.71–77.67 g) and yield per plant (513.3–1976 g). Cluster analysis for 10 quantitative traits grouped the 51 accessions into 6 clusters. Out of 61 SSR primers screened, 30 were polymorphic and highly informative as a means to differentiate these accessions. Based on genotyping, a high level of genetic diversity was observed, with a total of 99 alleles. The polymorphic information content (PIC) values ranged from 0.038 for marker BG_SSR-8 to 0.721 for S-24, with an average of 0.429. The numbers of alleles ranged from 2 to 5, with an average of 3.3 alleles per locus. Gene diversity ranged from 0.04 for BG_SSR-8 to 0.76 for S-24, showing a wide variation among 51 accessions. The UPGMA cluster analysis grouped these accessions into 3 major clusters. Cluster I comprised 4 small, fruited accessions that are commercially cultivated in central and eastern India. Cluster II comprised 35 medium- to long-sized fruited accessions, which made up an abundant and diverse group. Cluster III comprised 11 long and extra-long fruited accessions. The polymorphic SSR markers of the study will be highly useful in genetic fingerprinting and mapping, and for association analysis in *Momordica* regarding several economic traits.

Keywords: bitter gourd; population structure; genetic diversity; morphological traits; SSR marker



Copyright: © 2021 by the authors. Licensee MDPI, Basel, Switzerland. This article is an open access article distributed under the terms and conditions of the Creative Commons Attribution (CC BY) license (<https://creativecommons.org/licenses/by/4.0/>).

1. Introduction

Bitter gourd (*Momordica charantia* L. $2n = 2x = 22$), known as bitter melon or balsam pear, is an economically and horticulturally important multipurpose vegetable of the Cucurbitaceae family. Compared with other cucurbits, it is highly valuable for its nutritional content, providing carbohydrates, proteins, vitamins, minerals, and ascorbic acid [1], and for numerous medicinal uses [2]. The juice has been used for centuries in Ayurveda as an ancient traditional medicine for treating diabetes [3] and also possesses



Analytic approximate solutions of diffusion equations arising in oil pollution

Hijaz Ahmad^{a,*}, Tufail A. Khan^a, Hülya Durur^b, G.M. Ismail^{c,e}, Asif Yokus^d

^aDepartment of Basic Sciences, University of Engineering and Technology, Peshawar, 25000, Pakistan

^bDepartment of Computer Engineering, Faculty of Engineering, Ardahan University, Ardahan, 75000, Turkey

^cDepartment of Mathematics, Faculty of Science, Sohag University, Sohag, 82524, Egypt

^dDepartment of Actuary, Faculty of Science, Firat University, Elazig, 23200, Turkey

^eDepartment of Mathematics, Faculty of Science, Islamic University of Madinah, 170, Madinah, Saudi Arabia

Received 18 March 2020; received in revised form 26 April 2020; accepted 5 May 2020

Available online 2 June 2020

Abstract

In this article, modified versions of variational iteration algorithms are presented for the numerical simulation of the diffusion of oil pollutions. Three numerical examples are given to demonstrate the applicability and validity of the proposed algorithms. The obtained results are compared with the existing solutions, which reveal that the proposed methods are very effective and can be used for other nonlinear initial value problems arising in science and engineering.

© 2020 Shanghai Jiaotong University. Published by Elsevier B.V.

This is an open access article under the CC BY-NC-ND license. (<http://creativecommons.org/licenses/by-nc-nd/4.0/>)

Keywords: Modified variational iteration algorithm-II; Diffusion equation; Allen-Cahn equation; Parabolic equation; MVIA-I.

1. Introduction

Partial differential equations (PDEs) are studied in various fields such as astrophysics, fluid mechanics, solid-state physics, ocean engineering, plasma physics, optical fibre, wave motion, ocean ecology, and metrology and have been studied by many scientists for many years.

Oil pollution is the release of a fluid oil hydrocarbon into the ocean environment because of human activities such as releases of unrefined petroleum from tankers, drilling rigs, offshore platforms as well as piping and may cause serious damage to the marine ecological environment. Therefore, a precise guess of behaviours of these oils is extremely noteworthy to keep the seaside natural environmental system. The zone of oil spreading can be anticipated numerically by the solution of proper equations governing the flow field and the

diffusion phenomenon. The most reasonable choice is probably the diffusion equations where the information about the quantity of oil, which reached the ocean outlet can be taken as initial and boundary conditions for modelling of oil diffusion and alteration in the waters.

To describe oil pollution, consider the general nonlinear diffusion equation of the form:

$$\frac{\partial v}{\partial t} = \mathcal{D} \frac{\partial^2 v}{\partial x^2} + \alpha v + \beta v^n, \quad (1)$$

Where v is concentration, \mathcal{D} is diffusion coefficient, α and β are real constants. Eq. (1) becomes Allen-Cahn equation when $n = 3$, $\alpha = 1$ and $\beta = -1$, which has various applications in quantum mechanics, biology and plasma physics [1].

There are various analytical and numerical methods for the solution of nonlinear equations i.e. the finite difference method [2,3], Modified Kudryashov method [4], Sumudu transform method [5], $(1/G')$ -expansion method [6], expansion methods [7,8], finite element method [9], Hirota's bilinear method [10,11], Decomposition methods [12–15], variational iteration algorithm-I [16–20], function transformation

* Corresponding author.
E-mail addresses: hijaz555@gmail.com (H. Ahmad), tufailmarwat@uetpeshawar.edu.pk (T.A. Khan), hulyadurur@ardahan.edu.tr (H. Durur).

RESEARCH

Open Access



Application of triple compound combination anti-synchronization among parallel fractional snap systems & electronic circuit implementation

Emad E. Mahmoud^{1,2*} , Pushali Trikha³, Lone Seth Jahanzaib³, M. Higazy^{1,4} and Monagi H. Alkinani⁵

*Correspondence:

e.mahmoud@tu.edu.sa;
emad_eluan@yahoo.com

¹Department of Mathematics and Statistics, College of Science, Taif University, P.O. Box 11099, Taif 21944, Saudi Arabia

²Department of Mathematics, Faculty of Science, Sohag University, Sohag 82524, Egypt

Full list of author information is available at the end of the article

Abstract

In this article we examine the dynamical properties of the fractional version of the snap system by means of chaotic attractor, existence, and uniqueness of the solution, symmetry, dissipativity, stagnation point analysis, Lyapunov dynamics, K.Y. dimension, bifurcation diagram, etc. Also, parallel systems to this system are synchronized in presence of uncertainties and external disturbances using triple compound combination anti-synchronization by two ways. Synchronization time is compared with some other works. Also the utilization of achieved synchronization is illustrated in secure transmission. By constructing the snap system's signal flow graph and its real electronic circuit, some of its additional invariants are investigated.

Keywords: Dynamical properties; Electronic circuit; Parallel systems; Triple compound combination anti-synchronization

1 Introduction

Chaos is the common attribute of nonlinear dynamical systems. It has some interesting features such as irregular, complex, and unpredictable behavior. It was in 1960 while studying atmospheric turbulence that Lorenz [25, 26] realized that the 3-D differential equation system possessed a very irregular chaos like solution. After the Lorenz system, the Lu system and Chen system were proposed which too had complex dynamical behavior. In order to utilize chaos, many methods have been developed by researchers, such as chaos control, suppression, and synchronization, which led to the revolution in chaos theory. Because of these developments, chaotic systems found many applications across many disciplines such as secure communication, robotics, weather systems, encryption, neurons, circuits, oscillators, ecology, biology, and finance systems. Chaos synchronization, in which two or more chaotic systems are made to follow the same path on application of suitable controllers, was introduced in 1990. Synchronization of chaos involves synchronizing systems which are highly sensitive to initial conditions (I.C.) and parametric values. Many synchronization techniques [17, 19–22, 27, 30, 31, 35, 54] have been developed since then using various control methods. Table 1 gives an idea of how new synchronization

© The Author(s) 2021. This article is licensed under a Creative Commons Attribution 4.0 International License, which permits use, sharing, adaptation, distribution and reproduction in any medium or format, as long as you give appropriate credit to the original author(s) and the source, provide a link to the Creative Commons licence, and indicate if changes were made. The images or other third party material in this article are included in the article's Creative Commons licence, unless indicated otherwise in a credit line to the material. If material is not included in the article's Creative Commons licence and your intended use is not permitted by statutory regulation or exceeds the permitted use, you will need to obtain permission directly from the copyright holder. To view a copy of this licence, visit <http://creativecommons.org/licenses/by/4.0/>.

Assessment of Flood Hazard West of Sohag Governorate, Egypt

Mostafa Redwan^{1*}, Marwa Abo Amra¹, Ahmed A. Abdel Moneim¹, Ahmed M. Youssef^{1,2}

¹ Geology Dept. Faculty of Science, Sohag University, 82524 Sohag, Egypt

² Geological Hazards Department, Applied Geology Sector, Saudi Geological Survey, P.O. Box 54141, Jeddah 21514, Saudi Arabia

Received: 10 Jun. 2020, Revised: 16 Sep. 2020, Accepted: 7 Oct. 2020.

Published online: 1 Jan. 2021

Abstract: Although Egypt has limited rainfall events, flashfloods are responsible for huge losses of lives and infrastructure. In this study, the geomorphometric parameters of the hydrographic basins in the area west of Sohag city, Upper Egypt was carried out. Stream orders, lengths and numbers, bifurcation ratio, drainage frequency and density, circularity and elongation ratios for 16 drainage basins in the study area are quantified to develop a system for flood hazard assessment and mitigation using ESRI's ArcGIS 10.1. The similarities in the calculated bifurcation ratios of the studied basins indicate that the genetic conditions of the stream orders are the same for each basin. Drainage densities show that these basins were developed under almost the same climatological and hydrogeological conditions. Most of the basins (62%) showed moderate hazard possibility, 25% exhibit low hazard possibilities and wadis El-Kawamil Bahri and El-Shaykh El-Aqra exposed high hazard possibilities. Due to the establishment of new urban areas, industrial zones, land reclamation and different types of projects in the study area, it is recommended to build small dams on appropriate locations for areas with high-moderate hazard probability to protect it and restore the excess water derived from any runoff and could be used for cultivation.

Keywords: Geomorphometric parameters – Flashfloods – Hazard Potential – Bifurcation ratios – Sohag, Egypt.

1 Introduction

Characterizing and recognition the locations where hazardous processes are going to occur and their natural or human-induced return period (i.e., time between events) is of particular importance. [1] As a result, outlining the natural and human-induced hazards is environmental planning to avoid those locations where the hazards are most likely to occur and to zone the land appropriately. Also, carefully considering the important links between geologic processes, the environment, and society is required. The low desert zone in the study area (latitudes 26° 22' 00" and 26° 29' 30" N and longitudes 31° 31' 00" and 31° 41' 30" E) ((Figure 1) that surround Sohag governorate, acquire major development projects. These projects include; Sohag new city, the air port, the new extension of Sohag University, the West Gerga industrial zone, land reclamation of several hundred of feddan and the desert roads connecting Sohag to Assiut and Aswan. Therefore, analyzing and assessment of the natural hazards and recommending the means of protection in the area are of great importance. Unfortunately, these changes in the landuse and the establishment of forementioned projects have been carried out without proper consideration of the

geo-natural hazards in the area. [2] Thereto, the potential geo-environmental hazards that can occur in the area include flash floods; sand dune movement and drifting; swelling and shrinkage of clay deposits; karastification due to carbonate rocks dissolution; land subsidence and discharge of wastewater in open pits near urbanization. In this study, flash flood hazard assessment in the area and their impacts will be investigated.

Several factors has been found to affect flooding and vulnerability to public, these including changes in landuse, urbanization and squatter settlements and sub-standard constructions, and increased household density. [3] Flood hazards are controlled by different factors that include topography, geomorphology, drainage, engineering structures, and climate. Saleh stated the following factors that influence flood potentiality: rainfall and its characteristics, water loss (evaporation and infiltration), drainage basins, drainage networks, drainage orders, drainage characteristics, and environmental and human processes. [4] The average topographic elevation of the low desert zone in the study area ranging from 78-105 m above sea level. The old cultivated land about 68 m above sea level, surrounded from east and west by the limestone plateau with average elevation of 250 m. As a result a general slope from west to east. The plateau is intersected

* Corresponding author E-mail: mostafa.redwan@science.sohag.edu.eg

Biologically active organic compounds as insect growth regulators (IGRs): introduction, mode of action, and some synthetic methods

Mohamed A. Gad^{a*}, Safwat A. Aref^{a†}, Antar A. Abdelhamid^b, M. M. Elwassimy^b and Shaban A. A. Abdel-Raheem^c

^aResearch Institute of Plant Protection, Agriculture Research Center, 12112 Giza, Egypt

^bDepartment of Chemistry, Faculty of Science, Sohag University, 82524 Sohag, Egypt

^cSoil, Water, and Environment Research Institute, Agriculture Research Center, Giza, Egypt

CHRONICLE

Article history:

Received January 29, 2021

Received in revised form

April 11, 2021

Accepted May 31, 2021

Available online

May 31, 2021

Keywords:

Growth regulators

Synthesis

Mode of action

Insects

ABSTRACT

Biologically active organic compounds continue to attract great interest due to the wide variety of interesting applications observed for these compounds. This review results from the literature survey containing the organic compounds that are used as insect growth regulators with a focus on their mode of action and some synthetic routes.

© 2021 by the authors; licensee Growing Science, Canada.

1. Introduction

There is no doubt that there are many organic compounds with good biological and pharmacological activities.¹⁻¹⁵ Insect growth regulators (IGRs), also called third-generation insecticides, are pesticides that disrupt the normal activity of the endocrine or hormone system of the insects, affecting the development, reproduction, or metamorphosis of the target insect.¹⁶ Several features of insect growth regulators (IGRs) make them attractive as alternatives to broad-spectrum insecticides.¹⁷ Some of these features are more selective, less harmful to the environment, more compatible with pest management systems that include biological control,¹⁸ and less likely to be lost because of resistance. Insects have demonstrated a propensity to develop resistance to insecticides.¹⁹ Virtually all chemicals used to control insects fall into one of three categories: neurotoxins, growth regulators and behavior modifiers. Most chemicals used to control insects are neurotoxins which interfere with normal nerve function. Organophosphorus insecticides were derived from nerve gases that were first exploited for military purposes. Other insecticides were discovered by testing chemicals to find their insecticidal activities.²⁰ Among those that kill quickly is a neurotoxin acted on neurotransmissions was sought and developed as an insecticide. In the early discovery and development of insecticides, efforts were focused on chemistry rather than biology.²¹ Insect growth regulators (IGRs) are compounds that interfere with

* Corresponding author.

E-mail address: samy_adjev@yahoo.com (M. A. Gad)



Biomass derived P-containing activated carbon as a novel green catalyst/support for methanol conversion to dimethyl ether alternative fuel

Kamal M.S. Khalil^{a,*}, Walaa A. Elhamdy^a, Mohamed N. Goda^b, Abd El-Aziz A. Said^b

^a Chemistry Department, Faculty of Science, Sohag University, P.O. Box 82524, Sohag, Egypt

^b Chemistry Department, Faculty of Science, Assiut University, P.O. Box 71516, Assiut, Egypt

ARTICLE INFO

Editor: Dr. Z. Wen

Keywords:

Methanol
Dimethyl ether
Activated carbon
Green catalyst
Fuel

ABSTRACT

The current environmental situation has urged researchers to look for alternative green fuels with lower emissions from biomass feedstock. This work aims a greener approach for the heterogeneous catalytic conversion of methanol to dimethyl ether, DME, as an alternative fuel. Thus, a series of phosphorous-containing activated carbon (ACP) derived from orange peel (OP) at different H₃PO₄: OP (w/w) ratios, as well as a series of tungsten (W)-loaded on ACP, WO₃/ACP supported catalysts were formed and thermally treated at different temperatures. The formed materials were characterized by XRD, ATR-FTIR, N₂ adsorption/desorption, HRTEM, electron diffraction, EDX, elemental mapping and surface acidity. Effects of H₃PO₄ ratio and treatment temperature on the bulk and surface properties of the produced catalyst/support materials were investigated. Catalytic activities of the ACP support and W-loaded catalysts towards methanol dehydration in the range of 150–400 °C were measured at WHSV of 2.01 h⁻¹ in an inert atmosphere. Improved catalytic performance was observed for ACP support, which further improved for the W-loaded catalysts. This involved increase of methanol conversion (from 67% to 84%), DME formation rate (from 14.6 to 18.3 mmol.h⁻¹), time-on-stream (from < 40 to >120 h) and E_a (from 48.98 to 42.23 kJ mol⁻¹) on moving from ACP support to the most active supported catalyst, respectively. The improvement was attributed to the enhanced textural and thermal stability of the supported catalyst, which places it among the high efficiency catalysts for DME formation.

1. Introduction

Large number of recent researches has been devoted to converting of bio-based inedible residual agriculture materials into green catalysts/supports [1,2] green adsorbents [3,4] and bio/green fuels [4,5]. Dimethyl ether (DME) is one of the most promising renewable and environmentally friendly fuels [4,5]. Thus, DME is very suitable for diesel engines due to its high cetane number and can act as a source for H₂ production through catalytic steam reforming process that produces H₂ and CO₂ [6,7]. Moreover, DME ensures similar properties to propane and butane, the principal components of Liquefied Petroleum Gas (LPG) [8], therefore it can act as an alternative fuel for domestic application [9]. Notably, DME is able to pass the toughest emission regulations, due to its structure simplicity, very low emission of particulate matter and lower emission of toxic gases (such as NO_x and SO_x) compared with traditional diesel fuels [8,10]. Additionally, DME is a multi-purpose synthetic chemical material, which employed as a propellant gas and can substituted chlorofluorocarbons (CFCs) among a variety of

applications and can prevent damage of the ozone layer [11].

The use of biomass as feedstock to produce alternative fuels and chemicals is a central policy of today's society [12]. The synthesis of DME from biomass-derived feedstock may be achieved via catalytic dehydration of methanol, which is the main process for DME production; or from syngas (H₂ + CO/CO₂) via catalytic hydrogenation of carbon oxides. For catalytic methanol dehydration, solid acid catalysts such as alumina, γ-Al₂O₃ [8,13,14], and zeolites [15–17] have been widely employed as catalysts. However, γ-Al₂O₃ suffers from the possible preferential adsorption of water produced during the methanol dehydration reaction on the catalysts surface. Whereas, Zeolites possesses too strong acid sites that led to undesirable by-products and lowers the reaction formation yield. Therefore, It has been established that catalytic dehydration of methanol requires weak to moderate acid sites [10]. Thus, a variety of solid materials with controlled acidity have been developed for methanol dehydration such as nano sized SAPO11 [18], ferrierite nano crystals [19] and Pd₂Ga nanoparticle catalyst [20].

In an effort for more greener chemistry, activated carbon derived by

* Corresponding author.

E-mail addresses: kms_khalil@yahoo.co.uk, kms_khalil@sci.sohag.edu.eg (K.M.S. Khalil).

<https://doi.org/10.1016/j.jece.2021.106572>

Received 13 July 2021; Received in revised form 8 October 2021; Accepted 9 October 2021

Available online 16 October 2021

2213-3437/© 2021 Elsevier Ltd. All rights reserved.

Contents lists available at [ScienceDirect](https://www.sciencedirect.com)

Comparative Biochemistry and Physiology, Part C

journal homepage: www.elsevier.com/locate/cbpcBioremediation of hemotoxic and oxidative stress induced by polyethylene microplastic in *Clarias gariepinus* using lycopene, citric acid, and chlorellaAlaa El-Din H. Sayed^{a,*}, Mohamed Hamed^b, Ahmed E.A. Badrey^b, Hamdy A.M. Soliman^c^a Zoology Department, Faculty of Science, Assiut University, 71516 Assiut, Egypt^b Department of Zoology, Faculty of Science, Al Azhar University, Assiut Branch, 71524 Assiut, Egypt^c Department of Zoology, Faculty of Science, Sohag University, 8562 Sohag, Egypt

ARTICLE INFO

Edited by Martin Grosell

Keywords:

Microplastics
Poikilocytosis
Lycopene
Citric acid
chlorella

ABSTRACT

Despite extensive research on the toxic effects of microplastics (MPs), there is no obtainable data on the use of phytobioremediation against MPs toxicity in fish. This study aimed to investigate the protective role of lycopene, citric acid, and chlorella against the toxic effects of MPs in African catfish (*Clarias gariepinus*) using hematology, biochemical, antioxidants, erythron profiles (poikilocytosis and nuclear abnormalities) and the accumulation of MPs in tissues as biomarkers. Five groups of fish received: normal diet (control); MPs (500 mg/kg diet) (Group 2); MPs (500 mg/kg diet) + lycopene (500 mg/kg diet) (Group 3); MPs (500 mg/kg diet) + citric acid (30 g/kg diet) (Group 4); and MPs (500 mg/kg diet) + chlorella (50 g/kg diet) (Group 5) for 15 days. Group 2 had significantly higher amounts of MPs in the stomach, gills, and feces, electrolyte imbalances (HCO_3^- , Fe , Na^+ , K^+ , Ca^{+2} , Cl^- , and anion gap, hematobiochemical alterations, and decreases in the activities of superoxide dismutase, catalase, total antioxidant capacity, and glutathione S-transferases compared to the control group. Additionally, Group 2 had significant increase in the percentage of poikilocytosis, and nuclear abnormalities in RBCs compared to the control group. The co-treatment of MPs-exposed fish with lycopene, citric acid, and chlorella-supplemented diets ameliorated the hematological, biochemical, and erythron profile alterations, but only slightly enhanced the antioxidant activity. Overall, lycopene, citric acid, and chlorella can be recommended as a feed supplement to improve hematobiochemical alterations and oxidative damage induced by MPs toxicity in the African catfish (*C. gariepinus*).

1. Introduction

Microplastic (MPs) is defined as plastic debris consisting of ubiquitous tiny fragments, fibers, films, or particles that are smaller than 5 mm in diameter (Wright et al., 2013). The annual global demand for plastics has increased alongside population in recent years, with annual plastic production increased dramatically to 300 million tons (EuropePlastic, 2015). Egypt consumed approximately 2.1 million tons of polymers in 2017 and is the largest polymer consumer in Africa (Babayemi et al., 2019). This overconsumption of plastic combined with the absence of waste disposal management and uncontrolled plastic waste dumping in Egypt are causing severe impacts on aquatic ecosystems (Hamed et al., 2019a). Increased plastic production has resulted in widespread MPs pollution, which can have an enduring impact on the global environment, especially in aquaculture systems (Zhou et al., 2021). Most water sources contain MPs that directly or indirectly enter the aquaculture

systems before entering the body of the aquatic animals and finally entering food chain (Zhou et al., 2021). Aquaculture is currently the most important source of fish in Egypt and accounts for nearly 65% of Egypt's entire fish production, with more than 99% produced from privately owned farms (Kaleem and Sabi, 2020).

Several studies have reported that MPs can elicit ecotoxicological effects in fish, such as anemia, biochemical disturbance, and oxidative stress (Barboza et al., 2018; Choi et al., 2018; Hamed et al., 2019a, 2020; Lu et al., 2016; Qiao et al., 2019; Wang et al., 2019). Recently, active components from herbal plants have been explored as possible antioxidants in fish. Lycopene is a red-colored carotenoid present in many fruits and vegetables. Due to its high number of conjugated dienes, lycopene is one of the most potent antioxidants, with a singlet-oxygen-quenching ability that is twice that of β -carotene and 10 times that of α -tocopherol (Sahin et al., 2014). In many study, lycopene improved hepatorenal and hematological functions, and also reduced oxidative

* Corresponding author.

E-mail address: alaasayed@aun.edu.eg (A.E.-D.H. Sayed).<https://doi.org/10.1016/j.cbpc.2021.109189>

Received 15 June 2021; Received in revised form 3 September 2021; Accepted 6 September 2021

Available online 10 September 2021

1532-0456/© 2021 Elsevier Inc. All rights reserved.



Blueshifted dielectric properties and optical conductivity of new nanoscale nickel-(II)-tetraphenyl-21H,23H-porphyrin films as a function of UV illumination for energy storage applications

A. El-Denglawey^{1,2} · H. A. Alburaih³ · M. M. Mostafa^{4,5} · M. S. S. Adam^{6,7} · M. M. Makhlouf^{4,8}

Received: 16 July 2020 / Accepted: 22 May 2021 / Published online: 24 June 2021
© The Author(s), under exclusive licence to Springer Science+Business Media, LLC, part of Springer Nature 2021

Abstract





Pristine thermally evaporated nickel-(II)-tetraphenyl-21H,23H-porphyrin (NiTPP) thin films are amorphous, but after 4 and 8 h of UV illumination, the films become crystalline with preferred orientations of (112), (103) and (004) and crystallite sizes of (13, 18, 16) and (42, 31, 38) nm after 4 and 8 h, respectively. After UV illumination for 4 and 8 h, the NiTPP thin films are characterized by blueshifted absorption coefficients, increasing the optical and fundamental gap values and decreasing the dispersion parameter values. The dielectric properties display energy storage regions corresponding to the peak values of optical conductivity, which provides an elegant confirmation of the tailoring and tuning of band gaps, energy storage properties and optical conductivity by UV illumination time. Therefore, NiTPP films may be good candidates for environmental and energy storage applications.

Keywords Phase and optical properties · Energy conversion and storage · Photovoltaic system · Optical conductivity · Nanomaterials · Thin films

✉ A. El-Denglawey
a.denglawey@tu.edu.sa; denglawey@yahoo.com

- ¹ Physics Department, Turabah University College, Taif University, Turabah 21995, Saudi Arabia
- ² Nano & Thin Film Laboratory, Physics Department, Faculty of Science, South Valley University, Qena 83523, Egypt
- ³ Physics Department, Faculty of Science, Princess Nourah Bint Abdulrahman University, Riyadh, Kingdom of Saudi Arabia
- ⁴ Science & Technology Department, Rania University College, Taif University, Rania 12975, Kingdom of Saudi Arabia
- ⁵ Physics Department, Faculty of Science, Suez University, Suez, Egypt
- ⁶ Chemistry Department, Faculty of Science, King Faisal University, 380, Al Hassa-31982, Al Hofuf, Kingdom of Saudi Arabia
- ⁷ Chemistry Department, Faculty of Science, Sohag University, Sohag-82534, Egypt
- ⁸ Department of Physics, Damietta Cancer Institute, Damietta, Egypt

Boosting the catalytic performance of manganese (III)-porphyrin complex MnTSPP for facile one-pot green synthesis of 1,4-dihydropyridine derivatives under mild conditions

Mahmoud Abd El Aleem Ali El-Remaily¹  | Hesham A. Hamad^{2,3}  |
Ahmed M. M. Soliman¹  | Omar M. Elhady¹ 

¹Department of Chemistry, Faculty of Science, Sohag University, Sohag, Egypt

²Fabrication Technology Research Department, Advanced Technology and New Materials Research Institute (ATNMR), City of Scientific Research and Technological Applications (SRTA-City), New Borg El-Arab City, Alexandria, Egypt

³Biological and Chemical Research Centre, Faculty of Chemistry, University of Warsaw, Warsaw, Poland

Correspondence

Mahmoud Abd El Aleem Ali El-Remaily, Department of Chemistry, Faculty of Science, Sohag University-82524 Sohag, Egypt.
Email: msremaily@yahoo.com

Hesham A. Hamad, Fabrication Technology Research Department, Advanced Technology and New Materials Research Institute (ATNMR), City of Scientific Research and Technological Applications (SRTA-City), New Borg El-Arab City, Alexandria, Egypt.
Email: hhamad@srtacity.sci.eg

In this study, the metal complex (5,10,15,20-tetrakis-(4-sulfonatophenyl)-porphyrin manganese (III) chloride; denoted as MnTSPP) represents a promising efficient and reusable heterogeneous solid catalyst for facile and highly efficient one-pot synthesis of 1,4 dihydropyridine derivatives via three-component condensation reaction of aromatic aldehyde, ethyl acetoacetate, and ammonium acetate under green and mild reaction conditions. The simple operation, short reaction time (15 min), and the high efficiency (99%) are the special advantage of this protocol. Furthermore, the green aspects of this synthetic protocol were more studied by examination of the reusability of MnTSPP for four consecutive cycles without a significant loss of catalytic activity. Remarkably, the new synthesis presented advantages in terms of safety, commercially available catalyst, simplicity, stability, mild conditions, short reaction time, and excellent yields, using a mixture of H₂O and C₂H₅OH environmental-friendly solvent, operationally facile, wide tolerance of starting materials, and excellent recoverable of the catalyst.

KEYWORDS

1,4-dihydropyridines, benign protocol, manganese (III)-porphyrin complex, mild condensations; recoverable catalyst, three-component reaction

1 | INTRODUCTION

Metal-porphyrins have attracted more attention for broad applications in catalysis.^[1] Among these reactions, metal-porphyrins have a significant catalytic activity towards the oxidative processes in organic synthesis. So the development of catalysts is claiming huge attention due to their wide applications of the produced organic compounds with high selectivity and productivity.

It is well known that the porous metal-porphyrin networks have demonstrated to be an excellent technology in

the field of homogeneous and heterogeneous catalysis.^[2] The strategy of immobilization of porous metal-porphyrin (Figure 1) has already been developed by organic amorphous polymers, amorphous inorganic matrices, or crystalline inorganic materials such as silica,^[3] zeolites,^[4] clay from the smectite group (montmorillonite),^[5,6] layered double hydroxides,^[7,8] tubular and fibrous matrices,^[9] and silica matrix obtained by the sol-gel process.^[10-16]

The search for broadly applicable metal catalysts operating in the aqueous phase is a subject of high interest.^[17-19] Environmental applications of metal catalysis

Contents lists available at [ScienceDirect](https://www.sciencedirect.com)

Optik

journal homepage: www.elsevier.com/locate/ijleo

Original research article

Bures and trace-distance correlations of quantum wells in open microcavities linked by an optical waveguide

A.-B.A. Mohamed^{a,b,*}, M. Abdel-Aty^c, H. Eleuch^{d,e}^a Department of Mathematics, College of Science and Humanities in Al-Aflaj, Prince Sattam bin Abdulaziz University, Saudi Arabia^b Faculty of Science, Assiut University, Assiut, Egypt^c Mathematics Department, Faculty of Science, Sohag University, 82524 Sohag, Egypt^d Department of Applied Physics and Astronomy, University of Sharjah, United Arab Emirates^e Institute for Quantum Science and Engineering, Texas A&M University, College Station, TX77843, USA

ARTICLE INFO

Keywords:

Bures-norm entanglement
Measurement-induced non-locality
Microcavities

ABSTRACT

We explore the two quantum-wells correlations in two microcavities linked by a waveguide and leaking its photons to the external environment. Each microcavity contains quantum well (QW) and filled by a linear optical medium. We examine the effects of the physical parameters on the generation and robustness of the Bures-norm entanglement and the trace-norm measurement-induced non-locality correlation. The generations and the robustness of the Bures and trace-distance correlations depend crucially on the cavity-QW and fiber cavity couplings as well as on the optical linear medium density. The optical susceptibility, the spontaneous emission and the microcavity dissipation rates, in addition to the couplings of cavity-QW and the fiber-cavity control the regularity, amplitudes, and frequencies of the Bures and trace-distance correlations.

1. Introduction

One of the most intriguing subjects in quantum information and quantum computing is the physical understanding of quantum correlations (QCs), such as quantum entanglement (QE) [1], the geometrical quantifiers of non-locality and the discord [2], which have been extensively explored recently. In particular, the quantum correlations cannot correspond to a classical property exhibiting a variety of proprieties in bi- and multi-partite quantum system. Nowadays, quantum entanglement is considered as crucial to applications of quantum information, such as: computing [3], key distribution [4], teleportation [5], cryptography [6] and quantum memory [7,8].

Entanglement is not the only kind of QC that can exist in some mixed states. The system can be disentangled and still have quantum correlation [9,10]. Therefore, other QC quantifiers introduced as: quantum discord [9,11], measurement-induced disturbance [12], the geometrical quantifiers, geometric quantum discord and measurement-induced nonlocality (MIN) [13]. These quantifiers are used to investigate the QC in different physical models [14–16].

The Hilbert–Schmidt norm quantifiers have been proved to be inefficient QC measures [17]. Consequently, new measures were introduced based on quantum skew information [18,19] and others norms such as: Schatten one-norm (trace distance/trace norm)[20, 21] and Bures norm [22]. These norms pave the way for several geometric approaches to the quantification of quantum correlations.

* Corresponding author at: Department of Mathematics, * College of Science and Humanities in Al-Aflaj, Prince Sattam bin Abdulaziz University, Saudi Arabia.

E-mail address: abdelbastm@yahoo.com (A.-B.A. Mohamed).

<https://doi.org/10.1016/j.ijleo.2020.165744>

Received 12 August 2020; Received in revised form 30 September 2020; Accepted 30 September 2020

Available online 30 October 2020

0030-4026/© 2020 Elsevier GmbH. All rights reserved.

Changes in RAPD-DNA Markers and Plasma Protein Profile in Progesterone-Treated Chicken

Tito Naeem Habib¹, Gamal El-Din S. Amin¹, Ahmed Ahmed Hussien¹, Mohammed Salama²,
Mohamed Omar Ahmed¹, Motamed Elasyed Mahmoud^{3,*}

¹Molecular Genetics Lab, Department of Zoology, Faculty of Science, Sohag University, 82524, Egypt

²Department of Zoology, Faculty of Science, Ain Shams University, 11566, Egypt

³Department of Animal Behavior and Husbandry (Genetics, Breeding and Production),

Faculty of Veterinary Medicine, Sohag University, 82524, Egypt

*Corresponding author: motamed71111@gmail.com, moatamed_ali@vet.sohag.edu.eg

Received August 07, 2021; Revised September 10, 2021; Accepted September 22, 2021

Abstract The abuse of contraceptive pills as growth promoters in the poultry industry has serious health concerns. Consumption of hormonal residues in animal products results in reproductive disorders and an increased risk of cancers in humans. This study aimed to investigate the effect of treatment with progesterone hormone on the plasma proteins and RAPD-DNA markers of broiler chickens. One hundred, one-day-old broiler chicks were equally divided into 5 groups (n = 20). Four groups were treated daily with progesterone hormone either subcutaneously or orally (1.0 mg, 1.5mg/kg). The 5th group was control non-treated chicken. Sodium dodecyl sulfate polyacrylamide gel-electrophoresis (SDS-PAGE), and RAPD assays in conjunction with productive parameters such as growth rate were assessed. SDS-PAGE and RAPD-DNA patterns were significantly affected by progesterone hormone treatment. Either oral or subcutaneous progesterone hormone treatments increased the body weight of chicks compared to control. Treatment with progesterone hormone induces effects on both DNA and plasma proteins in broiler chickens. Changes at the genomic DNA level may be due to specific modifications in RAPD patterns or arise as a consequence of hot spot DNA changes and/or mutations.

Keywords: *Xeno-progesterone, plasma protein profile, RAPD-DNA markers, growth rate, broiler chicken*

Cite This Article: Tito Naeem Habib, Gamal El-Din S. Amin, Ahmed Ahmed Hussien, Mohammed Salama, Mohamed Omar Ahmed, and Motamed Elasyed Mahmoud, "Changes in RAPD-DNA Markers and Plasma Protein Profile in Progesterone-Treated Chicken." *Journal of Food and Nutrition Research*, vol. 9, no. 9 (2021): 477-483. doi: 10.12691/jfnr-9-9-4.

1. Introduction

Naturally occurring hormones, such as progesterone, oestrogen, and testosterone, are necessary for various physiological processes in animals and humans. These chemicals are excreted in urine and feces as metabolites or conjugated forms, leading to contamination of water, milk, and animal product, which are consumed directly or indirectly by humans, plants, and animals [1]. The carcinogenic and endocrine-disrupting potentials are the main health concerns associated with the use of hormonal compounds as growth promotants or therapeutic agents. Certainly, poultry, cow and horse manure contains the greatest amount of steroidal estrogens that may contaminate the environment [2]. Several reports confirm that diethylstilboestrol endangers the health of animals and humans when repeatedly used in large doses. Further, cooking or frozen storage did not affect the nature or quantity of their metabolites [3].

The six hormonal types most widely used in meat production include three natural hormones, oestradiol 17,

testosterone, and progesterone, and three synthetic substances, trenbolone, zeranol, and melengestrol acetate [4]. Although some studies indicated that estradiol-17 beta has the genotoxic potential [2]. Scientists of Joint FAO/WHO Expert Committee on Food Additives pointed out that no data are demonstrating that concentrations below the no-hormonal-effect level cause adverse effects in animals or humans [5]. Under their normal biochemical action, low concentrations of steroid hormones (nM) bind to and activate their intracellular receptors, which interact with hormone response elements in DNA, leading to the transcription of genes that induce cell proliferation and growth [6]. Therefore, a hormonal substance could promote carcinogenicity in hormone-sensitive tissues through such a proliferative mechanism [7,8]. Though receiving less attention, the other health concern is the endocrine-disrupting effects of hormonal growth promotants, notably their significant potential to perturb normal development in sensitive subpopulations like prepubertal children and developing fetuses [9].

Only limited new information was presented in the European Commission studies and other cited literature regarding the metabolism, endocrine-disrupting potential,



Changes in the morphological traits and the essential oil content of sweet basil (*Ocimum basilicum* L.) as induced by cadmium and lead treatments

Naglaa A. Youssef

To cite this article: Naglaa A. Youssef (2020): Changes in the morphological traits and the essential oil content of sweet basil (*Ocimum basilicum* L.) as induced by cadmium and lead treatments, International Journal of Phytoremediation, DOI: [10.1080/15226514.2020.1812508](https://doi.org/10.1080/15226514.2020.1812508)

To link to this article: <https://doi.org/10.1080/15226514.2020.1812508>



Published online: 30 Sep 2020.



Submit your article to this journal [↗](#)



Article views: 4



View related articles [↗](#)



View Crossmark data [↗](#)



Cite this: *CrystEngComm*, 2021, 23, 2835

Characterization of defect levels in β -Ga₂O₃ single crystals doped with tantalum

Haoyue Liu,^{ab} Naiji Zhang,^{ab} Junhua Yin,^a Changtai Xia,^{id}*^b Zhe Chuan Feng,^a Kaiyan He,^{*a} Lingyu Wan^{id}^a and H. F. Mohamed^{id}*^{bc}

We present a detailed study on the crystal structure of 0.10 mol% Ta-doped β -Ga₂O₃ crystals before and after annealing treatment in air by high-resolution X-ray diffraction and Raman spectroscopy, as well as the detection of point defects through the variation of photoluminescence excitation (PLE) and photoluminescence (PL) with temperature. Based on the experimental data, the band diagram of the 0.10 mol% Ta-doped β -Ga₂O₃ crystal is constructed. The crystal quality of the 0.10 mol% Ta-doped β -Ga₂O₃ crystal was improved after annealing treatment. The PL spectra exhibited two ultraviolet emission bands (UV ~3.59 eV, UV' ~3.22 eV) and a blue emission band (BB ~2.73 eV), which are ascribed to the recombination of self-trapped excitons at the trigonal O_I and O_{II} sites and gallium vacancies in the (2-) charge state (tetrahedral site), respectively. The work function of the 0.10 mol% Ta-doped β -Ga₂O₃ crystal increased from 5.28 eV to 5.38 eV as a result of annealing treatment.

Received 12th November 2020,
Accepted 2nd March 2021

DOI: 10.1039/d0ce01639j

rsc.li/crystengcomm

1. Introduction

Recently, beta gallium oxide has attracted great attention in research and development (R&D) due to its large bandgap (~4.9 eV), high breakdown electric field (~8 MV cm⁻¹), low cost and high quality to form large β -Ga₂O₃ single-crystal substrates, which makes it a promising candidate for optoelectronic devices.¹⁻⁶ β -Ga₂O₃ has a monoclinic structure with the space group *C2/m* and its unit cell consists of two nonequivalent Ga sites, which are tetrahedral and octahedral sites, and three nonequivalent O sites that are either trifold (O_I, O_{II}) or fourfold (O_{III}) coordinated.⁷

Previous studies revealed the photoluminescence of β -Ga₂O₃ with intrinsic ultraviolet (UV) and extrinsic blue-band (BB) emissions ascribed to the recombination of self-trapped excitons and donor-acceptor pairs, respectively.^{8,9} It was found that holes above the valence band tend to be localized by forming small polarons (GaO₄ tetrahedra) on a single O atom in the lattice, while free conduction electrons are trapped at single or coupled oxygen vacancies known as donors.

Tuning the carrier concentration and bandgap of semiconductors are essential to improve the performance of optoelectronics devices. Moreover, it has been observed that in some semiconductors, the energy gap decreases and the work function increases owing to the annealing treatment.¹⁰⁻¹²

It is known that the Ta ion has up to 5 valence electrons and its ionic radius (0.064 nm) is close to the ionic radius of Ga (0.062 nm). Thus, when Ga³⁺ ions are replaced by Ta⁵⁺ ions, it results in extra free electrons on the Ga₂O₃ lattice. This in turn leads to an increase in the electrical conductivity and infrared reflectivity of the β -Ga₂O₃ crystal.¹¹ Substitution of the Ga³⁺ ion with the Ta⁵⁺ ion can be expected not to cause the formation of structural defects due to its close ion radius. Additionally, a Ta-doped material is a promising material for obtaining high-performance photovoltaic solar cell (PSC) technologies.¹³ So far, there are only a few reports of Ta-doped β -Ga₂O₃ crystals or films. Due to the above, Ta can be considered a very suitable doping element for Ga₂O₃ crystals.

The current research is focused on the study of point defects of 0.10 mol% Ta-doped β -Ga₂O₃ crystals through the variation of photoluminescence excitation (PLE) and photoluminescence (PL) with temperature, as well as the effect of the annealing treatment on the optical properties and electronic structure.

2. Experimental

2.1 Crystal growth experiments

0.10 mol% Ta-doped β -Ga₂O₃ crystals were prepared using the optical floating zone method. The starting materials are β -Ga₂O₃ (6 N) and Ta₂O₅ (4 N) powders. The mixed powder was

^a Laboratory of Optoelectronic Materials & Detection Technology, Guangxi Key Laboratory for the Relativistic Astrophysics, School of Physical Science & Technology, Guangxi University, Nanning 530004, China.

E-mail: gredhky@gxu.edu.cn


^b Key Laboratory of Materials for High Power Laser, Shanghai Institute of Optics and Fine Mechanics, Chinese Academy of Sciences, Shanghai 201800, China.

E-mail: xia_ct@siom.ac.cn

^c Physics Department, Faculty of Science, Sohag University, 82524 Sohag, Egypt. E-mail: h.fathy@science.sohag.edu.eg



Cold RF oxygen plasma treatment of graphene oxide films

F. M. El-Hossary¹, Ahmed Ghitas², A. M. Abd El-Rahman^{1,3}, A. A. Ebnalwaled⁴,
M. Abdelhamid Shahat^{2,*} , and Mohammed H. Fawey¹

¹Physics Department, Faculty of Science, Sohag University, Sohag 82524, Egypt

²PV Unit, Solar and Space Research Department, National Research Institute of Astronomy and Geophysics (NRIAG), Helwan 11421, Cairo, Egypt

³King AbdulAziz University, Jeddah, Saudi Arabia

⁴Electronics & Nano Devices Lab, Physics Department, Faculty of Science, South Valley University, Qena 83523, Egypt

Received: 20 February 2021

Accepted: 3 May 2021

Published online:
17 May 2021

© The Author(s), under
exclusive licence to Springer
Science+Business Media, LLC,
part of Springer Nature 2021

ABSTRACT

Oxygen radio-frequency (RF) plasma technique is one of the most novel directions used to improve the physical and chemical properties of graphene oxide (GO). Herein, plasma treatment is used to enhance the chemical functionalization and reduced levels of the GO material for electronic and solar cell applications. GO films were chemically synthesized with high quality and uniformity. Then, they exposed to surface modification using RF oxygen plasma at a processing power of 100 W at different processing times. The microstructure and surface chemistry of the GO films were characterized by X-ray photoelectron spectroscopy (XPS) and Raman spectroscopy. Moreover, the effect of oxygen plasma on the thermal stability, surface roughness, contact angle, work of adhesion, wettability, spreading coefficient, and electrical properties have been studied. The results revealed a decrease in the amount of oxygen-containing groups (such as epoxides, carbonyls, and carboxyl groups) from 48.8% in pristine GO to 36.15% after 5 min of oxygen plasma treatment. Besides, the carbonyls groups (C = O) disappeared while new chemical bonds were created compared to the pristine GO film such as hybridized carbon atoms (SP³) and carboxyl's (O–C = O). Accordingly, the electrical conductivity increases from 0.11 S/m of pristine GO to an optimum value of 0.46 S/m after 5 min of plasma treatment, as a result of the incorporation of high amount of carboxyl, hydroxyl and carbonyl groups. The current results indicate that the properties of GO can be tuned by varying the degree of oxidation, which may pave the way for new developments in GO-based applications.

Address correspondence to E-mail: m.abdelhamid999@gmail.com



Comparative Study between *Croton tiglium* Seeds and *Moringa oleifera* Leaves Extracts, after Incorporating Silver Nanoparticles, on Murine Brains



CrossMark

Wael M. Aboulthana^{a,*}, Ahmed M. Youssef^b, Mohamed M. Seif^{c,d}, Noha M. Osman^e, Ram K. Sahu^f, Mohamed Ismael^g, Hatim A. El-Baz^a, Nagwa I. Omar^a

^a Biochemistry Department, Genetic Engineering and Biotechnology Research Division, National Research Centre, 33 El Bohouth St. (former El Tahrir St.), Dokki, Giza, P.O. 12622, Egypt.

^b Packaging Materials Department, National Research Centre, 33 El Bohouth St. (former El Tahrir St.), Dokki, Giza, P.O. 12622, Egypt.

^c Toxicology and Food Contaminants Department, Food Industries and Nutrition Research Division, National Research Centre, 33 El Bohouth St. (former El Tahrir St.), Dokki, Giza, P.O. 12622, Egypt.

^d College of Animal Science and Technology, Northwest A&F University, Yangling, Shaanxi, 712100, China.

^e Cell Biology Department, Genetic Engineering and Biotechnology Research Division, National Research Centre, 33 El Bohouth St. (former El Tahrir St.), Dokki, Giza, P.O. 12622, Egypt.

^f Department of Pharmaceutical Science, Assam University (A Central University), Silchar-788011, Assam, India.

^g Energy and Environmental Sciences Laboratory, Chemistry Department, Faculty of Science, Sohag University, Egypt.

Abstract

Croton tiglium seeds and *Moringa oleifera* leaves extracts are rich in phytoconstituents with the antioxidant efficiency which can be enhanced by incorporating silver nanoparticles (Ag-NPs). The present study was designed to compare the effect of *C. tiglium* seeds and *M. oleifera* leaves nano-extracts on brain tissues of murine models. During the current study, acetylcholine esterase (ACHE), β -amyloid (A β) content and inflammatory markers were measured in brain tissues. Moreover, native protein, lipoprotein and isoenzymes patterns were electrophoretically detected. Also, the interferon-gamma (INF- γ) receptor protein was studied by molecular dynamic simulation to evaluate the significant alterations on brain tissues. It was found that ACHE, A β contents and inflammatory markers increased in *C. tiglium* nano-extract treated group at a dose of 6.5 ml/kg. Furthermore, it caused qualitative electrophoretic abnormalities represented by lowering similarity index (SI) values. Also, the residues range 119–127 represent the most reactive and flexible site in INF- γ receptor protein. On the other hand, it was shown that no significant differences were induced by silver *M. oleifera* nano-extract.

Keywords: *Croton tiglium* Seeds; *Moringa oleifera* Leaves; Nanotechnology; Electrophoresis; Molecular Dynamic Modelling.

1. Introduction

Croton tiglium plays an effective role in ethnomedicine for treatment of several cancer diseases [1]. It belongs to the family Euphorbiaceae that includes about 280 genera and 8000 species [2]. Moreover, *C. tiglium* seeds extracts are rich in various active phytochemicals such as ascorbic acid, tocopherol and other pigments. All these phytoconstituents are responsible for the antioxidant efficiency of the plant extract [3].

It is well known that *C. tiglium* seeds are characterized by the presence of phorbol esters,

crotonic acid, fatty acids and active phytoconstituents, which are responsible for severe purgative effect of the *C. tiglium* seeds extract [4]. In addition to, croton oil which is rich in 12-O-tetradecanoylphorbol-13-acetate and exhibits the most effective role in inhibiting growth and stimulating apoptosis in solid tumors [5]. On the other hand, a study by El-Kamali *et al.* [6], reported that aqueous *C. tiglium* seeds extracts have no significant alterations in the biochemical

*Corresponding author e-mail: wmkamel83@hotmail.com.; (Wael M. Aboulthana).

Receive Date: 15 December 2020, Revise Date: 31 December 2020, Accept Date: 03 January 2021

DOI: 10.21608/EJCHEM.2021.53777.3113

©2021 National Information and Documentation Center (NIDOC)



Comparison of different adsorption pairs based on zeotropic and azeotropic mixture refrigerants for solar adsorption ice maker

Massaud Mostafa^{1,2} · M. Ezzeldien^{3,4} · M. Attalla⁵ · Nouby M. Ghazaly⁵ · Z. A. Alrowaili¹ · M. F. Hasaneen^{1,6} · Ahmed N. Shmroukh⁵

Received: 3 December 2020 / Accepted: 15 March 2021 / Published online: 30 March 2021
© The Author(s), under exclusive licence to Springer-Verlag GmbH Germany, part of Springer Nature 2021

Abstract

One of the important ways to the efficiently use of low-grade thermal energy is the adsorption refrigeration technology. However, it has some drawbacks such as low specific cooling power and coefficient of performance, especially under using the conventional adsorption pairs. Therefore, new adsorption pairs are tested in solar adsorption ice-maker and compared with other conventional pairs data from open literature to find the tendency of improving the solar adsorption ice-maker performance. The experimental test rig has been built in Upper Egypt in Qena City. Four different new adsorption pairs of granular activated carbon/R-410A, granular activated carbon/R-511A, Maxsorb III/R-410A, and Maxsorb III/R-511A are used. It is demonstrated that Maxsorb III/R-511A pair based solar adsorption ice-maker produced the highest values for specific cooling power, coefficient of performance, and ice production per 1 kg of adsorbent of approximately 226.7 W/kg_{ads}, 0.197, and 1.96 kg/kg_{ads}, respectively. While granular activated carbon/R-410A based solar adsorption ice-maker produced the lowest values of ice production per 1 kg of adsorbent and coefficient of performance of 1.38 kg/kg_{ads} and 0.104, respectively. Moreover, it can be concluded that the tested pairs are feasible to be used in solar adsorption ice-maker systems, especially in such hot climate of Upper Egypt for food and vaccine preservation and storage.

Keywords Adsorption refrigeration · Solar ice-maker · COP · Ice production · Freshwater

Introduction

Growing energy resources consumption in many cities around the world is one of the main results of urbanization and social

development. Air condition and refrigeration systems consume a considerable part of the total electricity generation around the world (Akbari et al. 2020). However, such systems are essential to be used in harsh environmental conditions of

Highlights

- New adsorption pairs were applied to solar adsorption ice-maker.
- Using Maxsorb III/R-511A pair in solar adsorption ice-maker is promising.
- The coefficient of performance of the proposed ice-maker reached up to 0.197.
- Ice production of the proposed ice-maker increased to reach up to 1.96 kg/kg_{ads}.
- Food and vaccine storage can be attained by the proposed solar adsorption ice-maker.

Responsible Editor: Philippe Garrigues

✉ Ahmed N. Shmroukh
eng_ahmednagah@yahoo.com

¹ Department of Physics, College of Science, Jouf University, Sakaka 2014, Saudi Arabia

² Department of Physics, Faculty of Science, South Valley University, Qena 83523, Egypt

³ Department of Basic Sciences, Common First Year Deanship, Jouf University, P.O. Box: 2014, Sakaka, Saudi Arabia

⁴ Metallurgy & Material Science Tests (MMST) Lab, Department of Physics, Faculty of Science, South Valley University, Qena, Egypt

⁵ Department of Mechanical Engineering, Faculty of Engineering, South Valley University, P.O. Box 83521, Qena 83521, Egypt

⁶ Department of Physics, Faculty of Science, Sohag University, Sohag 82524, Egypt

Materials Science inc. Nanomaterials & Polymers

Condensation of Active Methylene and Substituted Aldehydes over Mesoporous Nickel Oxides Nanostructures: A Combined Experimental and DFT Study

Mohamed Khairy,* Mounir Mohamed, and Mohamed Ismael^[a]

Mesoporous NiO nanoarchitectures (NAs) with controlled hexagonal platelet- and flower-like morphology were synthesized using facile hydrothermal methods in different reaction conditions. The NiO NAs were characterized by scanning electron microscopy (SEM), transmission electron microscopy (TEM), N₂ adsorption /desorption isotherms, and wide-angle X-ray diffraction. It was found that controlled morphology, large surface areas, and high crystallinity of NiO NAs offered high

catalytic reactivity toward Knoevenagel condensation reactions. Large reaction yields in an aqueous media and easy separation of the NiO NAs without losing the catalytic activity were observed. Further, the formation mechanism of $-C=C-$ bonds over NiO NAs surface was explored by density functional theory (DFT). These findings open a new avenue for efficient $-C=C-$ bonds formation using reusable NiO NAs catalyst without using any expensive solvents.

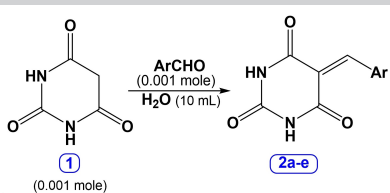
Introduction

The formation of $-C=C-$ bond has attracted much attention in organic chemistry not only for the synthesis of new compounds that has double bonds but also allows the introduction of several functional groups.^[1] Knoevenagel condensation is one of the classical and interesting organic reactions in the formation of $-C=C-$ bonds through the reaction of activated methylene compounds and substituted aldehydes.^[2] The formed alkene products are highly promising intermediates for synthesis of several organic molecules such as heterocyclic compounds, natural products, anti-hypertensive drugs, coumarin derivatives, perfumes, and cosmetics.^[3] The Knoevenagel condensation reaction is commonly performed in organic solvents in presence of bases such as primary or secondary amines and/or their salts. Although homogenous base catalyst i.e. KOH, NaOH, and alkali carbonates are effectively used, heterogeneous catalyst allows easy separation and management, facile recovery of products, and easily recycled. Numerous heterogeneous catalysts such as NaAlO₂,^[4] Na₂S/Al₂O₃,^[5] Cu(II)-Fe₃O₄ nanoparticles decorated melamine-functionalized chitosan,^[1] metal-organic framework (MOF)-NH₂,^[6] MOF-Pd,^[7] PMOV1,^[8] Zn@ZIF-67,^[9] ZIF-8,^[10] Cd(II) and Ni(II)-based coordination polymers,^[11] PdAlO(OH),^[12] titanosilicates,^[13] MCM-41 silica,^[14] and NiO NPs^[15] were utilized in Knoevenagel condensation reactions. However, time-consuming synthesis processes (i.e. microwave irradiation or ultrasonication), harsh reaction environmental conditions, toxic and expensive solvents or chemicals, and low catalyst reusing

impede their use in large-scale manufacturing. Therefore, exploring a green, efficient and reusable heterogeneous catalyst for formation of $-C=C-$ through condensation of active methylene and substituted aldehydes is highly desirable.

Mesoporous NiO nanostructures with different morphologies including hexagonal nanoplatelets (NPLs) and nanoflowers (NFs) are synthesized *via* simple and reproducible hydrothermal approaches and explored for Knoevenagel condensation reactions as shown in Tables 1 and 2. The NiO nanoarchitectures (NAs) with large-surface-area were produced and revealed high reaction yields of 98% in aqueous media. Although NiO-NFs showed a lower yield than NiO NPLs, it offered easy separation of solid *via* the magnetic characteristic of NiO NFs. The key to this achievement is that the NiO nanoarchitectures exhibit exceptional catalytic features for Knoevenagel in an aqueous environment without using any toxic or expensive solvents with considerable reaction yields.

Table 1. The condensation reaction of aromatic aldehydes and barbituric acid is catalyzed by NiO NAs.



Entry	Ar	Reaction time (min)	Yield (%) NiO NPLs	Yield (%) NiO NFs	MP: (°C) ^[17,18]
2a	C ₆ H ₅ -	15	92	75	263–265
2b	4-Cl-C ₆ H ₄ -	10	96	80	300–302
2c	4-MeO-C ₆ H ₄ -	8	98	82	296–298
2d	4-Me-C ₆ H ₄ -	10	95	78	290–292
2e	4-NO ₂ -C ₆ H ₄ -	12	90	70	272–274

[a] Dr. M. Khairy, Prof. M. Mohamed, Prof. M. Ismael
Chemistry Department, Faculty of Science, Sohag University, Egypt,
82524 Sohag
E-mail: mohamed.khairy@science.sohag.edu.eg

Supporting information for this article is available on the WWW under
<https://doi.org/10.1002/slct.202100675>



Constraints of Mantle and Crustal Sources Interaction during Orogenesis of Pre- and Post-collision Granitoids from the Northern Arabian-Nubian Shield: A Case Study from Wadi El-Akhder Granitoids, Southern Sinai, Egypt

Moustafa M. MOGAHED^{1,*} and Khaled M. ABDEL FADIL²

¹ *Geology Department, Faculty of Science, Benha University, Benha 13518, Egypt*

² *Geology Department, Faculty of Science, Sohag University, Sohag 82524, Egypt*

Abstract: The Egyptian older and younger granitic rocks emplaced during pre- and post-collision stages of Neoproterozoic Pan-African orogeny, respectively, are widely distributed in the southern Sinai Peninsula, constituting 70% of the basement outcrops. The Wadi El-Akhder, southwestern Sinai, is a mountainous terrain exposing two granitoid suites, namely the Wadi El-Akhder Older Granites (AOG) and the Homra Younger Granites (HYG). The AOG (granodiorites with subordinate tonalite compositions) have geochemical characteristics of medium-K calc-alkaline, metaluminous to mildly peraluminous granitoids formed in an island-arc environment, which are conformable with well-known Egyptian older granitoids rocks, whereas the HYG display calc-alkaline to slightly alkaline nature, peraluminous syeno-, monzogranites and alkali feldspar granites matching well those of the Egyptian younger granites. With respect to the AOG granitoids, the HYG granites contain lower Al₂O₃, FeO*, MgO, MnO, CaO, TiO₂, Sr, Ba, and V, but higher Na₂O, K₂O, Nb, Zr, Th, and Rb. The AOG are generally characterized by enrichment in LILE and LREE and depletion in HFSE relative to N-MORB values (e.g., negative Nb and Ta anomalies). The geochemical features of the AOG follow assimilation-fractional crystallization (AFC) trends indicative of extensive crustal contamination of magma derived from a mantle source. The chemical characteristics of the AOG are remarkably similar to those of subduction-related granitoids from the Arabian-Nubian Shield (ANS). The compositional variations from monzogranites through syenogranites to alkali feldspar granites within HYG could not be explained by fractional crystallization solely. Correlating the whole-rock composition of the HYG to melts generated by experimental dehydration melting of meta-sedimentary and magmatic rocks reveals that they appear to be derived by extended melting of psammitic and pelitic metasediments, which is similar to the most of younger granitic suites in the ANS.

Key words: older and younger granitoids, mantle-crust interaction, assimilation-fractional crystallization (AFC), southern Sinai, Arabian-Nubian Shield

Citation: Mogahed and Abdelfadil, 2021. Constraints of Mantle and Crustal Sources Interaction during Orogenesis of Pre- and Post-collision Granitoids from the Northern Arabian-Nubian Shield: A Case Study from Wadi El-Akhder Granitoids, Southern Sinai, Egypt. *Acta Geologica Sinica* (English Edition), 95(5): 1527–1550. DOI: 10.1111/1755-6724.14769

1 Introduction

Basement outcrops in Sinai Peninsula, southern Israel and southern Jordan, comprise the northernmost part of the Arabian-Nubian Shield (ANS). The ANS was evolved through four main stages. The oceanic, island arcs and plutonic rocks were formed during the subduction stage (~950–850 Ma; Bendor, 1985; Stern and Hedge, 1985; Stern and Manton, 1987; Kroner et al., 1990; Genna et al., 2002; Johnson and Woldehaimanot, 2003). The continental collision (~850–650 Ma; Avigad and Gvirtzman, 2009; Be'eri-Shlevin et al., 2009) resulting from continuing convergence between East and West Gondwana formed the East African orogen (Stern, 1994a). The post-collision stage (~650–580 Ma) marks stabilization of the shield and is characterized by

widespread calc-alkaline magmatism, mainly of intermediate to felsic composition and the occurrence of a vast peneplain (Avigad et al., 2005; Avigad and Gvirtzman, 2009). The last stage (~600–530 Ma; Fleck et al., 1980; Gass, 1981; Roobol et al., 1983; Bendor, 1985; Brown, 2015) representing late to post-orogenic within-plate magmatism is characterized by the severe igneous activity represented by alkaline to peralkaline granites.

A suite of syn- to post-tectonic tonalites, granodiorites and granites was emplaced throughout the Arabian-Nubian Shield between 690 Ma and 520 Ma (Bendor, 1985; Stern and Hedge, 1985; Genna et al., 2002; Johnson and Woldehaimanot, 2003). Although the precise timing of individual arc-arc collisions which constructed the Arabian-Nubian Shield between 715 Ma and 610 Ma is poorly known (Pallister et al., 1988), some of the 690–610 Ma granites, and many of the 610–520 Ma granites, are probably collision-related. They seem to have been

* Corresponding author. E-mail: mustafa.ahmed01@fsc.bu.edu.eg



Correlation between Raman spectra of $\text{Sn}_{1-x}\text{Fe}_x\text{O}_2$ nanoparticles and their electrical and magnetic properties

A.M. Abdel Hakeem^{a,*}, S.A. Saleh^{a,b}, E.M.M. Ibrahim^a

^a Physics Department, Faculty of Science, Sohag University, Sohag 82524, Egypt

^b Physics Department, College of Science & Arts, Najran University, P.O. 1988, Najran, Saudi Arabia

ARTICLE INFO

Keywords:

Fe doped SnO_2
Raman spectra
Electrical properties
Magnetic properties
Density

ABSTRACT

$\text{Sn}_{1-x}\text{Fe}_x\text{O}_2$ ($x = 0.00, 0.1, 0.12, 0.16$ and 0.18) nanoparticles have been synthesized by ball milling. Analyses of the Raman spectra exhibit a strong correlation between the internal structure of the nanoparticles and their electrical and magnetic properties. The blue shift in the peak position of the symmetric A_{1g} (630 cm^{-1}) mode as well as appearance of new two E_u modes (255 and 324 cm^{-1}) with Fe doping indicate to a formation of bridge oxygen vacancies in the nanoparticles which has been explained by Kröger–Vink notation. Oxygen vacancies make as trapping centers of the free electrons leading to an increase in the electrical resistivity. Fe doping induces another new peak at 540 cm^{-1} assigned to vibrations related to the Fe^{2+} ions accompanied by oxygen vacancies. The strength of this Raman peak increases with increasing the concentration of Fe in a good correlation with the behavior of the magnetization of the nanoparticles.

1. Introduction

Tin dioxide is a well-known wide band gap n-type semiconductor. It has a tetragonal rutile structure with four oxygen atoms and two tin atoms [1]. Sn atom is at the center of six oxygen atoms located at corners of regular octahedrons and each oxygen atom is surrounded by three Sn atoms at the corners of equilateral triangle. The O–Sn and O–O distances are 3.76 and 4.66 Å, respectively [2]. SnO_2 has various outstanding properties such as high optical transparency, electrical conductivity, and thermal and chemical stabilities [3–5] which make it a promising candidate for many multifunctional applications in gas sensors, solar cells, gas discharge, lithium ion batteries, light emitting diodes, transparent conducting electrodes, flat panel displays, spintronic devices, architectural glasses, aircraft glasses, etc. It has been reported that doping with transition metals can tune the internal structure and morphology as well as the electrical, structural, magnetic and optical properties of SnO_2 to find the way to various applications that require room temperature ferromagnetism (RTFM), high optical transparency, electrical conductivity, and chemical sensitivity [6–8].

The previously published results show that both the transition metal (TM) type and concentration have significant effects on the magnetic and electrical properties of SnO_2 resulting from the variation in the structure and defect density that associate the doping process [2,6–8].

For example, Sharma et al. [9] showed that substitution of Sn ions by Fe ions in SnO_2 lattice distorts the host lattice leading to a change in the magnetic and electrical properties due to the mixed valency nature of Sn and Fe cations. It was reported by Saleh et al. [10] that the band gap of the Fe doped SnO_2 nanoparticles decreases with increasing the Fe content. Similar behavior was reported by Ahmed et al. [11] for the optical band gap and attributed to formation of donor energy levels in SnO_2 . High Curie temperature ($\sim 500\text{ K}$) was reported by Fitzgerald et al. [12] in Co, Ni, Fe, Cr and Mn doped SnO_2 thin films at relatively lower doping level ($< 1\%$). They observed ferromagnetic ordering which might be intrinsic and caused by lattice and electronic defects created in the thin films. Also, SnO_2 doped with Fe and Co at higher level (3 and 5%) exhibited a single-phase tetragonal structure and room temperature ferromagnetic (FM) ordering with size-dependent phase transition temperature and saturation magnetization values as was reported by Kaur et al. [13]. Indeed, many research groups observed FM ordering in the pure and TM-doped SnO_2 and correlate between the magnetic properties and the surface defects of the SnO_2 nanostructures. However, Sharma et al. [2] reported that pure SnO_2 nanoparticles (average size = 20–25 nm) are nonmagnetic even with the existence of oxygen vacancies while a ferromagnetic ordering can be obtained only if the Fe concentration exceeds a ratio of 1% in the SnO_2 nanoparticles (NPs). Accordingly, they confirmed that intrinsic ferromagnetism (d^0 -magnetization)

* Corresponding author.

E-mail address: ahmedhakeem75@yahoo.com (A.M. Abdel Hakeem).

<https://doi.org/10.1016/j.mseb.2020.115025>

Received 10 August 2020; Received in revised form 29 November 2020; Accepted 21 December 2020

Available online 4 January 2021

0921-5107/© 2020 Elsevier B.V. All rights reserved.

Received 2 February 2021

Accepted 5 February 2021

Edited by W. T. A. Harrison, University of
Aberdeen, Scotland

Keywords: crystal structure; 3,3,6,6-tetra-
methyltetrahydroacridine-1,8-dione; C—H···O
hydrogen bonds; O—H···O hydrogen bonds;
acridines.

CCDC reference: 2061379

Supporting information: this article has
supporting information at journals.iucr.org/e

Crystal structure and Hirshfeld surface analysis of ethyl 2-[9-(2-hydroxyphenyl)-3,3,6,6-tetramethyl-1,8-dioxo-2,3,4,4a,5,6,7,8a,9,9a,10,10a-dodecahydroacridin-10-yl]acetate

Omyma A. A. Abd Allah,^a Manpreet Kaur,^b Mehmet Akkurt,^c Shaaban K. Mohamed,^{d,e*} Jerry P. Jasinski^b and Sahar M. I. Elgarhy^f

^aChemistry Department, Faculty of Science, Sohag University, 82524 Sohag, Egypt, ^bDepartment of Chemistry, Keene State College, 229 Main Street, Keene, NH 03435-2001, USA, ^cDepartment of Physics, Faculty of Sciences, Erciyes University, 38039 Kayseri, Turkey, ^dChemistry and Environmental Division, Manchester Metropolitan University, Manchester M1 5GD, England, ^eChemistry Department, Faculty of Science, Minia University, 61519 El-Minia, Egypt, and ^fFaculty of Science, Department of Bio Chemistry, Beni Suef University, Beni Suef, Egypt. *Correspondence e-mail: shaabankamel@yahoo.com

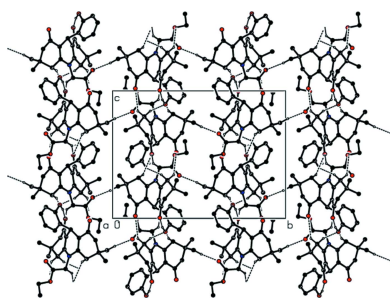
In the title compound, C₂₇H₃₃NO₅, a 3,3,6,6-tetramethyltetrahydroacridine-1,8-dione ring system carries an ethyl acetate substituent on the acridine N atom and an *o*-hydroxyphenyl ring on the central methine C atom of the dihydropyridine ring. The benzene ring is inclined to the acridine ring system at an angle of 80.45 (7)° and this conformation is stabilized by an intramolecular O—H···O hydrogen bond between the hydroxy substituent on the benzene ring and one of the carbonyl groups of the acridinedione unit. The ester C=O oxygen atom is disordered over major and minor orientations in a 0.777 (9):0.223 (9) ratio and the terminal —CH₃ unit of the ethyl side chain is disordered over two sets of sites in a 0.725 (5):0.275 (5) ratio. In the crystal, C—H···O hydrogen bonds combine to link the molecules into a three-dimensional network. van der Waals H···H contacts contribute the most to the Hirshfeld surface (66.9%) followed by O···H/H···O (22.1%) contacts associated with weak hydrogen bonds.

1. Chemical context

Acridine derivatives occur in a number of compounds of importance in medicinal chemistry such as bucrinae, which used for surface anesthesia of the eye and given by injection for infiltration anesthesia, peripheral nerve block and spinal anesthesia (Ramesh *et al.*, 2012). Quinacrine, also known as mepacrine, is used as a gametocytocide and acts as an anti-malarial agent (Valdés, 2011). Proflavin is also found to be active as a bacteriostatic agent (Patel *et al.*, 2010) and nitracrine is as anticancer agent (Cholewinski *et al.*, 2011). Acriflavin is used as an antiseptic for skin and mucous membranes (Ramesh *et al.*, 2012). As part of our studies in this area, we report herein the synthesis and crystal structure of the title compound, C₂₇H₃₃NO₅.

2. Structural commentary

As shown in Fig.1, the 3,3,6,6-tetramethyltetrahydroacridine-1,8-dione ring system carries an ethyl acetate substituent on the acridine N1 atom and an *o*-hydroxyphenyl ring on the central methine C7 atom of the C1/C6–C8/C13/N1 dihydropyridine ring. The acridinedione ring system deviates signifi-



OPEN ACCESS

Received 12 January 2021

Accepted 23 February 2021

Edited by C. Schulzke, Universität Greifswald,
Germany**Keywords:** crystal structure; cyclohexene ring;
dihydropyridine ring; hexahydroquinoline ring;
dimer.**CCDC references:** 2064688; 2064687**Supporting information:** this article has
supporting information at journals.iucr.org/e

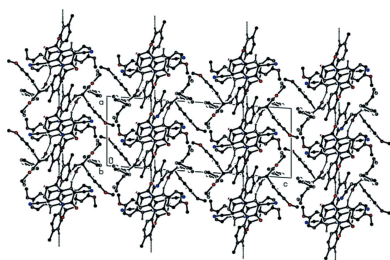
Crystal structures of 1-(4-chlorophenyl)-4-(4-methylphenyl)-2,5-dioxo-1,2,5,6,7,8-hexahydroquinoline-3-carboxylic acid and 4-(4-methoxyphenyl)-1-(4-methylphenyl)-2,5-dioxo-1,2,5,6,7,8-hexahydroquinoline-3-carbonitrile

Omyma A. Abd Allah,^a Manpreet Kaur,^b Mehmet Akkurt,^c Shaaban K. Mohamed,^{d,e,*} Asmaa H. A. Tamam,^a Sahar M. I. Elgarhy^f and Jerry P. Jasinski^b^aChemistry Department, Faculty of Science, Sohag University, 82524 Sohag, Egypt, ^bDepartment of Chemistry, Keene State College, 229 Main Street, Keene, NH 03435-2001, USA, ^cDepartment of Physics, Faculty of Sciences, Erciyes University, 38039 Kayseri, Turkey, ^dChemistry and Environmental Division, Manchester Metropolitan University, Manchester M1 5GD, England, ^eChemistry Department, Faculty of Science, Minia University, 61519 El-Minia, Egypt, and ^fFaculty of Science, Department of Bio Chemistry, Beni Suef University, Beni Suef, Egypt. *Correspondence e-mail: shaabankamel@yahoo.com

In the title compounds $C_{23}H_{21}ClN_2O_3$ [**I**, namely 1-(4-chlorophenyl)-4-(4-methylphenyl)-3,8-dioxo-1,2,5,6,7,8-hexahydroquinoline-3-carboxylic acid] and $C_{24}H_{22}N_2O_3$ [**II**, namely 4-(4-methoxyphenyl)-1-(4-methylphenyl)-2,5-dioxo-1,2,5,6,7,8-hexahydroquinoline-3-carbonitrile], each of the cyclohexene and dihydropyridine rings of the 1,2,5,6,7,8-hexahydroquinoline moieties adopts a twisted-boat conformation. The asymmetric units of both compounds **I** and **II** consist of two independent molecules (*A* and *B*). In **IIA**, three carbon atoms of the cyclohexene ring are disordered over two sets of sites in a 0.670 (11):0.330 (11) occupancy ratio. In the crystal of **I**, molecules are linked through classical $N-H\cdots O$ hydrogen bonds, forming inversion dimers with an $R_2^2(8)$ ring motif and with their molecular planes parallel to the crystallographic (020) plane. Non-classical $C-H\cdots O$ hydrogen-bonding interactions connect the dimers, resulting in a three-dimensional network. In the crystal of **II**, molecules are linked by $C-H\cdots N$, $C-H\cdots O$ and $C-H\cdots\pi$ interactions, forming a three-dimensional network.

1. Chemical context

Quinoline and its derivatives have for some time attracted the attention of both synthetic and biological chemists as a result of their diverse chemical and pharmacological properties (Kumar *et al.*, 2009). There are a number of natural products bearing the quinoline skeleton that are used as a medicine or employed as lead molecule for the development of new and potent therapeutics (Venkat Reddy *et al.*, 2009). Quinoline derivatives fused with various heterocycles have already demonstrated potent anticancer activity (Afzal *et al.*, 2015). In addition, it has been found that various quinoline compounds show anti-tuberculosis (TB) activity (Muscia *et al.*, 2014), anti-inflammatory activity (Psomas & Kessissoglou, 2013), anti-convulsant effects (Guo *et al.*, 2009), and anti-malarial parasite effects (Abdel-Gawad *et al.*, 2005). Furthermore, quinolones have been proved to be very effective in many antimicrobial and antioxidant investigations (Praveen *et al.*, 2010). In this context, we report herein the crystal structures of two derivatives of hexahydroquinoline.



OPEN ACCESS

Development of New Thiazole Complexes as Powerful Catalysts for Synthesis of Pyrazole-4-Carbonitrile Derivatives under Ultrasonic Irradiation Condition Supported by DFT Studies

Mahmoud Abd El Aleem Ali El-Remaily,* Tarek El-Dabea, Mohammed Alsawat, Mohamed H. H. Mahmoud, Alia Abdulaziz Alfi, Nashwa El-Metwaly,* and Ahmed M. Abu-Dief*



Cite This: *ACS Omega* 2021, 6, 21071–21086



Read Online

ACCESS |



Metrics & More

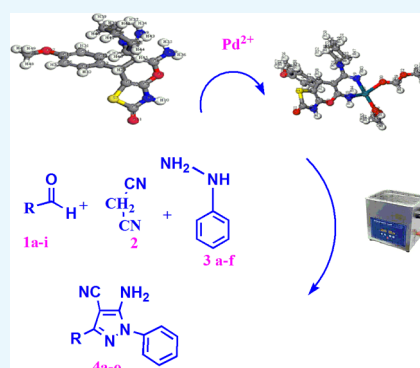


Article Recommendations



Supporting Information

ABSTRACT: In this study, we are interested in preparing Fe(III), Pd(II), and Cu(II) complexes from new thiazole derivatives. All syntheses were elaborately elucidated to estimate their molecular and structural formulae, which agreed with those of mononuclear complexes. The square-planer geometry of Pd(II) complex (MATYPd) was the starting point for its use as a heterocatalyst in preparing pyrazole-4-carbonitrile derivatives **4a–o** using ultrasonic irradiation through a facile one-pot reaction. The simple operation, short-time reaction (20 min), and high efficiency (97%) were the special advantages of this protocol. Furthermore, this green synthesis strategy was advanced by examination of the reusability of the catalyst in four consecutive cycles without significant loss of catalytic activity. The new synthesis strategy presented remarkable advantages in terms of safety, simplicity, stability, mild conditions, short reaction time, excellent yields, and use of a H₂O solvent. This catalytic protocol was confirmed by the density functional theory (DFT) study, which reflected the specific characteristics of such a complex. Logical mechanisms have been suggested for the successfully exerted essential physical parameters that confirmed the superiority of the Pd(II) complex in the catalytic role. Optical band gap, electrophilicity, and electronegativity features, which are essential parameters for the catalytic behavior of the Pd(II) complex, are based mainly on the unsaturated valence shell of Pd(II).



1. INTRODUCTION

Heterocyclic compounds of pyrazoles class are known by their importance in pharmaceutical targets and medicinal interest. Organic derivatives enriched by S and/or N atoms have a broad spectrum of biological activities such as antimicrobial, antioxidant,^{1,2} anti-HIV, anticancer,³ anticonvulsant,⁴ antimalarial, anti-inflammatory,⁵ and antidepressant.⁶ The ultrasonic state increases the rate of organic changes in mild conditions that otherwise require strict pressure and temperature conditions.⁷ Ultrasonic irradiation is also used to promote the formation, growth, and implosive collapse of bubbles in a liquid⁸ by various synthesis reactions. Initiated by cavitation, bubble collapse causes high stresses, extreme local heating, and very short lifetimes. Cavitation acts as a way of focusing the sound's scattered energy.^{9,10} Ultrasound irradiation can cause several reactions by providing activation energy, in contrast to traditional heating that provides thermal energy in the macro system.^{10a} Other benefits of ultrasound irradiation include high product yields, low reaction times, minimization of side products,^{10b} and nontoxic and environment-friendly solvents,¹¹ saving money and energy.

Previously variable methods involved synthesis of many pyrazole-4-carbonitrile derivatives via the one-pot multicomponent reaction (MCR) among arylaldehydes, malononitrile, and

phenylhydrazine using appropriate catalysts.¹² The significance of such compounds and relevance of such timely topics in organic synthesis were the use of ionic liquids¹³ and the need for green reaction approaches.¹⁴ The benefit of pyrazoles in drug designing has continuously trapped the pursuit for novel and advanced methods.¹⁵ Therefore, a novel protocol with a good and inexpensive catalyst demanding short reaction times is well desired.^{16,17}

In any of the abovementioned previous studies, pyrazole-4-carbonitrile derivatives catalyzed by new Pd(II) complexes under mild conditions have not been reported. Coinciding with outlined strategies and continuation of our work, we intended to achieve another success in the catalytic history of Pd(II) complexes by synthesizing bioactive heterocyclic compounds via multicomponent reactions. Because of the merits of being environmentally benign, readily accessible, and cost-effective,

Received: May 29, 2021

Accepted: July 23, 2021

Published: August 8, 2021

